Valorisation of SWRO brines in a remote island through a circular approach: Techno-economic analysis and perspectives

C. Morgante [a], F. Vassallo [a], D. Xevgenos [c,d,*], A. Cipollina [a], M. Micari [e], A. Tamburini [a,b,*], G. Micale [a]

[a] Dipartimento di Ingegneria, Università degli Studi di Palermo, viale delle Scienze Ed. 6, 90128 Palermo, Italy
[b] ResourSEAs SrL, viale delle Scienze Ed.16, 90128 Palermo, Italy
[c] Faculty of Applied Sciences, Delft University of Technology, Lorentzweg 1, 2628 CJ Delft, the Netherlands
[d] SEALEAU, Rotterdamsweg 183 C, 2629 HD Delft, the Netherlands
[e] Laboratory of Advanced Separations (LAS), Ecole Polytechnique Federale de Lausanne (EPFL), Sion, Switzerland

HIGHLIGHTS

- An innovative process for seawater reverse osmosis brine treatment was proposed.
- Recovery of high-quality water and salts: $Mg(OH)_2$, $Ca(OH)_2$ and NaCl.
- Optimized nanofiltration membranes allowed to recover high-purity table salt (97 %).
- Economic feasibility of the innovative process was demonstrated.
- Brine disposal costs more competitive than conventional disposal methods.

GRAPHICAL ABSTRACT
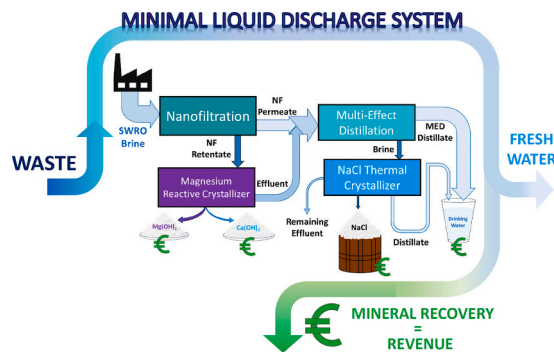
ARTICLE INFO

ABSTRACT

Nowadays, small remote islands rely heavily on desalination technologies to overcome freshwater scarcity. Unfortunately, these technologies are accompanied by the production of brines which can affect the receiving water bodies i.e., the aquatic ecosystem. Yet, it is extremely appealing how such brines constitute an abundant source of valuable raw materials (such as magnesium). In this work, a novel hybrid system is introduced to capture the value of seawater reverse osmosis (SWRO) brines produced in the minor Sicilian island of Pantelleria. The "Minimal Liquid Discharge" (MLD) process consists of: (i) Nanofiltration NF (separation of bivalent from monovalent ions), (ii) Mg Reactive Crystallizer MRC (selective recovery of magnesium and calcium), (iii) Multi-Effect Distillation MED (freshwater production) and (iv) NaCl Thermal Crystallizer NTC (sodium chloride recovery). The economic and environmental performances of the process have been evaluated by implementing and integrating the techno-economic models of each unit in a simulation platform called RCE (Remote Component Environment). Results revealed important economic benefits in comparison to conventional brine disposal methods. In addition, the proposed MLD chain turned out to be an attractive alternative for the production of high purity minerals/salts, achieving lower selling prices than the current market price.

---

* Corresponding author at: Dipartimento di Ingegneria, Università degli Studi di Palermo, viale delle Scienze Ed.6, 90128 Palermo, Italy.
E-mail addresses: D.Xevgenos@tudelft.nl (D. Xevgenos), alessandro.tamburini@unipa.it (A. Tamburini).

1. Introduction

Over the last decades, attempts to overcome freshwater scarcity are to be mostly associated with the installation of numerous desalination plants worldwide. Approximately 19,000 desalination plants are currently installed in the world, producing about 100 million m^3/day of freshwater [1]. More than half of such amount (65.5 million m^3/day) is produced exclusively by reverse osmosis (RO) [2]. Energy demand and the production of an effluent called "brine" [3] are the current drawbacks of current desalination technologies. As far as SWRO is concerned, meanwhile energy consumption has been decreased dramatically throughout the years (from approximately 16 kWh/m^3 in the 1970s to approximately 3 kWh/m^3 in 2020) [1], brine production, is still an issue to be tackled. Recent reviews estimate a global brine production of about 142 million m^3/day [4]. Brine is a solution that presents large amounts of total dissolved salts (TDS), and that must be necessarily treated before its discharge into the environment according to strict regulations [5]. When discharged, brine can be harmful to the environment due to its salinity, temperature and chemical substances (used for pre-treatment/ membrane cleaning). More specifically, brine salinity can be 1.6–2 times higher than that of seawater (35 g/L) [6] reaching up to 70 g/l [7] in the case of SWRO.

Current conventional brine management methods employed are: (i) ocean disposal [8], (ii) surface water discharge [9] (the least expensive of brine disposal methods [10]), (iii) sewer disposal [11], (iv) deep-well injection [3,12] and (v) evaporation ponds [3,13]. The choice of the disposal method to employ depends on several factors such as the quality, the volume, the location of the discharge point of the brine and the cost which typically lies within the range 5–33 % of the total cost of the desalination process [14]. Such disposal methods, however, are generally characterized by high capital costs, negative environmental impact or even both. Therefore, lower-cost and sustainable solutions are much needed [15].

To this aim, many schemes have been proposed in the last years aiming at the development of Zero Liquid Discharge (ZLD) systems or Minimal Liquid Discharge (MLD) systems that eliminate or diminish the discharge of liquid effluents, respectively, leading to the production of a solid waste to be disposed in landfill. Whereas ZLD processes consist of technologies integrated in such a manner to reach a water recovery of 95–99 %, MLD processes concern the integration of thermal and/or membrane-based processes reaching water recoveries around 80 % [16]. More recently, ZLD and MLD systems have undergone an evolution towards the additional recovery of valuable minerals (present in seawater brines [7]) in addition to freshwater. In this way, the waste to be disposed is transformed into a non-conventional resource of minerals to be fully exploited. In literature, several schemes based on this new concept of the ZLD/MLD strategy have been proposed and their techno-economic feasibility has been assessed. Recently, Panagopoulos [17] presented two SWRO brine valorisation chains, given by different combinations of nanofiltration, reverse osmosis, a brine concentrator (BC) and a brine crystallizer (BCr). Such chains could produce NaCl, a mixture of salts and reach water recoveries >99 %. Results of an economic evaluation showed that a water production cost of 1.04–1.37 $/$m^3$ could be achieved. The same author also proposed other two integrated chains: one based on reverse osmosis, a brine concentrator and wind-aided intensified evaporation (WAIV), the other based on reverse osmosis, a brine concentrator and a brine crystallizer, recovering solid salt and producing freshwater at a cost of 0.99 $/$m^3$ and 1.01 $/$m^3$, respectively [18]. In both works, no information concerning the purity of the recovered products were reported. Ji et al. [19] considered to treat SWRO brines via a membrane distillation unit (MD) and a crystallizer (Cr), reaching water recoveries up to 90 %. However, no economic analysis to prove its feasibility was carried out. Chen et al. [20] tested a multi-effect distillation unit integrated with a crystallizer to recover salt and water from desalination brine. Simulation results revealed that when waste heat was employed, a brine treatment cost of 4.17 $/$m^3$

could be obtained. Lower brine treatment costs (1.16 $/$m^3$) were reported when NaCl was recovered from brine via a supercritical water desalination technology introduced by Van Wyk et al. [4]. The promising latter two brine treatment costs, however, were given based on the sale of a generic product (NaCl) without a specific purity.

Furthermore, more complex ZLD systems capable of recovering different salts other than NaCl are also present in the literature. Al Bazedi et al. [21] identified a resource recovery scheme from brines comprising a chemical precipitation step and a membrane crystallizer (MCr). By adding $NaCO_3$, $CaCO_3$ was recovered, whereas NaCl, $MgSO_4$ and water were produced via membrane crystallization. More than 234 m^3/d of water could be produced with a revenue equal to 241,408 $/yr. This meant that a water specific production cost of 2.82 $/$m^3$ could be obtained. High revenues due to the sale of the other products were also reported. Nevertheless, purity and therefore possible applications of the final products were not specified. Turek et al. studied the recovery of Mg (OH)$_2$, $CaCO_3$ and freshwater via a chain constituted of electrodialysis (ED), chemical precipitation, ion exchange (IEX) and membrane electrolysis (ME) [22]. Subsequently, the same authors proposed to recover Mg(OH)$_2$, $CaSO_4$ and freshwater by means of electrodialysis, electrodialysis reversal (EDR) and Ca(OH)$_2$ treating [23]. Zhang et al. [24] investigated the performances of the integration of chemical precipitation, selectrodialysis (SED) and electrodialysis with bipolar membranes (BMED). Chemicals were produced, such as NaOH (85 % pure) and HCl (95 % pure), together with coarse salt (at a purity of 92 %). No economic evaluation, however, was conducted to demonstrate the feasibility of the production of the high purity chemicals. Kieselbach et al. [25] performed an economic investigation of a more complex ZLD chain based on nanofiltration, electrodialysis, evaporation (Ev), crystallization and membrane distillation. The chain was able to produce sodium hydrogen carbonate at a purity of 90 %, achieving a low brine disposal cost of 0.5 €/m^3. A much lower brine disposal cost (0.08 $/$m^3$) was obtained by Von Eiff et al. [26], by selling freshwater and pure Na_2SO_4, produced via the chain composed of membrane distillation, Multi Stage Flash (MSF) and Crystallization.

Within the framework of resource recovery from desalination brines, several European-funded projects have brought to life pilot-scale plants based on solar-powered evaporator-crystallizer systems. For example, within the SOL-BRINE project (project aiming at the development of a solar-driven brine treatment chain to eliminate the current practice of brine disposal), a system was developed to recover 90 % of water and dry salts from a pilot plant in Tinos Island (Greece). The plant was made of an evaporator, a crystallizer unit and a dryer unit employing solar collectors [3,27,28]. Similar projects such as AQUA-SOL and ZELDA proposed other ZLD systems based on the same concept.

All in all, for many proposed schemes present in literature, feasibility is not demonstrated due to the absence of a detailed economic analysis. In addition, for those cases in which an economic evaluation has been conducted, the schemes are capable of recovering water with a mixture of salts or one/two salts characterized by low purity. This meant that the price at which the recovered salts could be sold had to be necessarily low and the applications/target market of the same salts was very much limited.

Bearing this in mind, this work aims at filling such gap in the literature by conducting a detailed techno-economic analysis of an innovative and versatile brine valorisation chain capable of recovering water and three different single salts at very high purity (H_2O (TDS < 10 ppm), Mg(OH)$_2$ (>90 %), Ca(OH)$_2$ (>90 %) and NaCl (97 %)). This can be fully observed in Table 1, in which this work is compared with other works present in literature, based on brine valorisation schemes.

By achieving high purities, the products of our chain can target a much broader market than other ZLD/MLD schemes. Furthermore, among the recovered resources, Magnesium is one of the Critical Raw Materials (CRMs) defined by the European Union (EU) due to its very high supply risk. Therefore, both an economic benefit (recovery of high valuable minerals and water, lower cost for brine disposal) and an

Table 1

Comparison between proposed MLD chain and other brine valorisation schemes present in the literature.

Authors	Ref.	Feed	Valorisation chain	Recovery of multiple high purity minerals	Economic analysis	Levelized cost of minerals/water	Brine treatment specific cost
Panagopoulos	[17]	SWRO brine	RO-BC-BCr	✗	✓	✓	✗
Panagopolous	[17]	SWRO brine	NF-RO-BC-BCr	✗	✓	✓	✗
Zhang et al.	[24]	SWRO brine	Cr-SED-BMED	✓	✗	✗	✗
Panagopoulos	[18]	SWRO brine	RO-BC-BCr	✗	✓	✓	✗
Panagopoulos	[18]	SWRO brine	RO-BC-WAIV	✗	✓	✓	✗
Kieselbach et al.	[25]	SWRO brine	NF-ED-Ev-Cr-MD	✗	✓	✗	✓
Chen et al.	[20]	SWRO brine	MED-Cr	✗	✓	✗	✓
Von Eiff et al.	[26]	SWRO brine	MD-MSF-Cr	✓	✓	✗	✓
Van Wyk et al.	[4]	Hydrothermal brine	SCWD	✗	✓	✗	✓
Turek et al.	[23]	Coal mine brine	ED-EDR-Ca(OH)$_2$ treatment	✗	✗	✗	✗
Turek et al.	[29]	Coal mine brine	NF-Ev-Cr	✗	✗	✗	✗
Turek et al.	[22]	Coal mine brine	ED-Cr-IEX-ME	✗	✗	✗	✗
Ji et al.	[19]	SWRO brine	MD-Cr	✗	✗	✗	✗
Al Bazedi et al.	[21]	SWNF brine	Cr-MCr	✗	✓	✓	✗
Morgante et al. (this paper)	–	SWRO brine	NF-MRC-MED-NTC	✓	✓	✓	✓

Fig. 1. Sataria SWRO Plant, Pantelleria (IT).

Table 2

Ions concentrations of the brine produced by Sataria desalination plant obtained via ionic chromatography.

	Ionic species						
	Na$^+$	Ca^{2+}	Mg^{2+}	K$^+$	Cl$^-$	SO$_4^{2-}$	HCO$_3^-$
Concentration [g/l]	21.4	0.88	2.70	0.78	39.0	5.50	0.18

environmental one (reduction of brine discharge) can be achieved.

In this work, more specifically, an innovative brine management chain based on the MLD approach is investigated both technically and economically for a particular case study: treatment of the SWRO brine produced in the minor Sicilian island of Pantelleria (Italy). The idea is to propose a versatile brine treatment chain that can inspire industries to possibly implement it at an industrial scale. Therefore, a detailed techno-economic analysis was performed via a modelling platform, namely RCE [30], containing the mathematical models to simulate the treatment technologies. The results have been collected also with the support of PHREEQC thermodynamic equilibrium study [31]. The analyses allowed to find the best operating conditions that could maximize

the techno-economic feasibility and sustainability of the MLD chain proposed.

2. Case study and treatment chain description

In this paper, a seawater desalination plant located in Pantelleria was taken into examination. In particular, the brine produced by the Sataria seawater desalination plant was the object of the case study studied in this work [32]. A picture of the pressure vessels and high-pressure equipment of the RO plant is shown in Fig. 1.

The plant is made up of 4 RO units, each one with a capacity of 1250 m^3/d of freshwater produced. However, typically, only three of the four modules operate contemporarily meaning a daily average total capacity of about 3750 m^3/d. Each module presents an average water recovery of about 45 %. As previously discussed, an economic and environmental problem of seawater desalination is the production of brines (generally TDS = 70 g/l for a SWRO brine). The ionic concentration values of the brine produced by Sataria are reported in Table 2.

The main goal of the present work is to propose an innovative, environmentally and economically attractive MLD chain to valorise around 50 % of the total brine produced by the three operating RO modules of the "Sataria" SWRO plant.

The proposed treatment chain is illustrated in Fig. 2. As it is possible to observe, it consists of 4 units: (i) Nanofiltration NF, (ii) Mg Reactive Crystallizer MRC, (iii) Multi-Effect Distillation MED and (iv) NaCl Thermal Crystallizer NTC. The SWRO brine is fed to a nanofiltration unit that generates two different streams: a retentate rich in bivalent ions such as SO$_4^{2-}$, Ca^{2+} and Mg^{2+} and a permeate with a much lower concentration of the latter ions. The retentate is sent to an MRC in which magnesium and calcium are recovered in the form of hydroxide precipitates via a chemical reaction between the NF retentate and an alkaline reactant. The remaining effluent of the chemical reactor is mixed with the NF permeate and is fed to the MED unit. The latter concentrates the brine via evaporation within its multiple effects producing a distillate. Contemporarily, the MED reduces the brine volume that exits the unit at a salt concentration near that of saturation. The outlet brine is then sent to a final NTC in which NaCl precipitates forming a solid crystal product, a distillate and a remaining brine. The attractive aspect of the chain is that, starting from a waste brine, it is possible to reduce its volume therefore its environmental impact by producing many valuable products (Mg(OH)$_2$, Ca(OH)$_2$, drinking water and NaCl).

To better understand (i) the principles that lie at the core of the functioning of each technology and (ii) the reasons why the previous
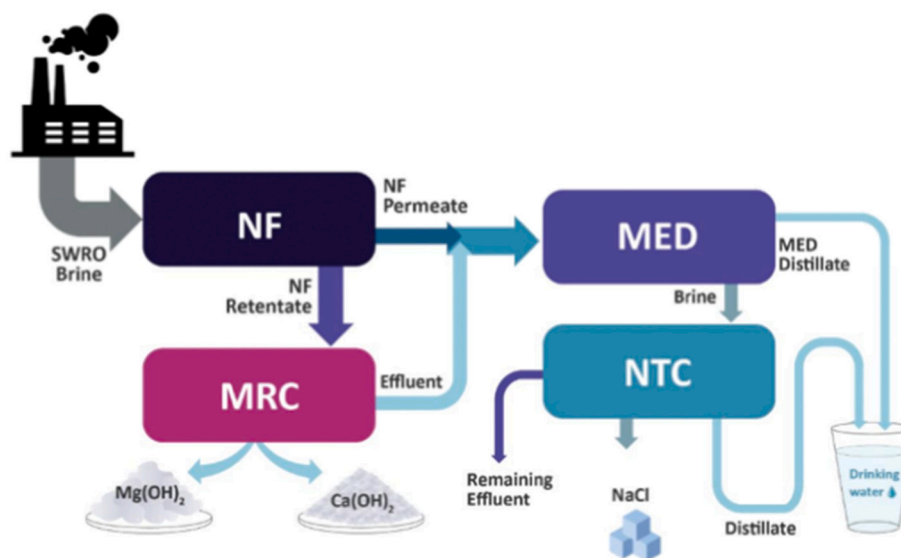
Fig. 2. Conceptual scheme of the proposed MLD system.

technologies were taken into consideration, details of each unit are reported in the following sections.

2.1. Nanofiltration (NF)

Nanofiltration is a pressure-driven membrane-based process usually applied nowadays as a pre-treatment technology in the desalination field [33]. The membrane employed presents properties in between those of RO and UF (Ultrafiltration) [34] with pore sizes that range from 1 to 2 nm [35]. Operating at low to moderate pressures levels (5–40 bar [36]) with permeate recoveries up to 80 % [37], NF presents higher water fluxes than RO and higher rejections than UF for small solutes [38]. The unique feature of NF is its capacity to reject bivalent ions such as Mg^{2+}, Ca^{2+} and SO_4^{2-} (60–99 % [39]) with a much higher selectivity than that for monovalent ions such as Na^+ and Cl^- (0–50 % [39]) [40]. Such behaviour is mainly due to the transport mechanisms that occur within the NF membrane based on (i) Steric hindrance (size-based exclusion), (ii) Dielectric exclusion (transport resistance due to an energy barrier associated with the shedding of the solute hydration) and (iii) Donnan exclusion (rejection/attraction due to membrane potential) [33]. The main drawback, as in any membrane process, is membrane fouling. However, NF has been widely tested in long-term runs demonstrating operational stability and improving overall performances of conventional desalination technologies such as RO, MSF and MED. More specifically, this was demonstrated by Saline Water Conversion Corporation (SWCC), achieving increases in water recovery (by 30 %) and overall reduction of energy consumption for NF-SWRO and NF-MSF/MED [36]. In particular, the presence of NF allowed to reduce scaling potential within MSF and MED and therefore to operate at higher temperatures (up to 120–130 °C) [41]. NF can be considered to be a good alternative to conventional pre-treatment technologies i.e., chemical precipitation. The latter requires large quantities of chemicals [42] and lacks robustness when brine concentrations tend to fluctuate. Furthermore, when compared to other membrane processes such as RO and FO (Forward Osmosis), higher energy consumption of the former and higher membrane cost of the latter are all factors that have led the author to believe that NF is the best option for the 1st step of the proposed MLD process.

2.2. Magnesium Reactive Crystallizer (MRC)

The Magnesium Reactive Crystallizer (MRC) operation consists of a direct mixing where the brine enters in intimate contact with an alkaline solution (NaOH). During the direct mixing of the two solutions,

magnesium ions (present in the brine) react with the hydroxyl ions of the alkaline solution, promoting precipitation of magnesium hydroxide crystals. However, the chemical reaction occurs at a pH value equal to 10.35. For a specific brine flow rate, there will be a specific alkaline flow rate required to reach the chemical reaction pH value. Other than magnesium recovery, it is possible to recover calcium as calcium hydroxide in a second stage. This second reaction, however, occurs at a higher pH value (precisely 13). Once magnesium and calcium have been recovered from the initial waste brine, the brine undergoes a neutralization step via HCl addition to restore the initial pH value of the brine. As an alkaline reactant, NaOH must be employed to ensure a high purity of magnesium hydroxide crystals. The use of NaOH for mineral recovery has been extensively tested in the past [43] capable of guaranteeing high purity products. On the other hand, other alkaline compounds, such as calcium hydroxide ($Ca(OH)_2$) or lime (dilute $Ca(OH)_2$ solution), have been found to cause the co-precipitation of by-products (i.e. calcium sulphates, carbonates and hydroxides) reducing the purity of magnesium hydroxide [44]. The functioning of the MRC mimics that of the pilot-scale plant "Multiple Feed — Plug Flow Reactor", developed and tested in real conditions by the same authors of the present work. High purity of $Mg(OH)_2$ and $Ca(OH)_2$, was experimentally demonstrated by the authors in previous works, reaching values higher than 90 % for both products [45,46]. Finally, a Drum filter is employed to recover magnesium and calcium hydroxide crystals from the outlet suspension of the MRC.

2.3. Multiple-Effect Distillation (MED)

Multi-Effect Distillation is a thermal-based technology widely employed in the desalination industry, capable of treating high salinity feeds. Even though it is the oldest [47], nowadays it remains the least energy consuming among the thermal-based technologies in use (i.e. MSF [48]), with values around 145–230 MJ/m³ of thermal energy [49]. MED consists of a series of evaporators, namely effects, that operate at decreasing pressures and temperatures from the first to the last effect [50]. The progressive reduction of pressure from one effect to another allows to diminish the temperature at which evaporation can occur. Each effect presents a tube bundle in which vapour flows transferring energy and on whose surface the feed is sprayed. Partial evaporation occurs producing (i) vapour that acts as the thermal vector of the following effect and (ii) remaining brine that is fed to the following effect. The produced vapour of the last effect is then condensed to a final distillate. Typical effects of an industrial MED can range from 2 to 16

[49] (depending on a series of factors), reaching even 20 in some cases [51]. The Top Brine Temperature TBT (the maximum temperature of the brine within the first effect) is limited to 60–90 °C due to scaling formation on the tube surfaces [52]. The presence of NF enables to increase the TBT up to 120–130 °C. Moreover, higher temperatures mean more effects, therefore a larger quantity of distillate. However, the number of effects is limited since minimum temperature differences between consecutive effects must be respected. Various MED configurations exist today: Backward feed, Forward feed, Parallel feed, Parallel/cross feed. For the techno-economic analysis, a forward feed configuration will be taken into account in order to reach high concentrations [53]. An MED process was developed at pilot scale and demonstrated also within the SOL-BRINE project [27]. The results from the SOL-BRINE project have shown that the TDS of the brine effluent can be increased up to the saturation point (26 %) of the sodium chloride, while recovering water of demineralized quality [28]. However, in such high concentration ratios the number of effects is limited compared to conventional MED desalination systems; with 5–10 effects being a more realistic value. Among the already mentioned advantages, the high quality of freshwater produced (TDS < 10 ppm), large capacity, possibility to treat high salinity feeds, concentration potential and robustness have led the author to use MED as the concentration step of the case study. Moreover, drawbacks such as low thermal efficiency [54] will be offset by the use of waste heat supplied by a near diesel power plant in Pantelleria.

2.4. NaCl Thermal Crystallizer (NTC)

As far as the production of NaCl is concerned, an evaporative crystallizer was selected: a very simple and common technology that enables to complete salt concentration up to saturation and promote NaCl precipitation via thermal energy. Contemporarily, a distillate and remaining brine are produced. It has been previously demonstrated in literature how an MED-evaporator, the combination of two conventional technologies, presents greater benefits than other alternative emerging processes for salt production from brines (i.e. Membrane Distillation) [20]. Other advantages such as the large capacities and possibility to use low grade/waste heat guided the authors' decision in choosing a crystallization technology. Due to a parametric analysis of the upstream technologies of the proposed MLD system carried out by the authors (see Section 6.1), the evaporative crystallizer was able to produce high purity NaCl (97 %), suitable for food purposes.

3. Technical models

The main objective of the work was focused on evaluating the feasibility of the proposed MLD treatment chain from a technical and economic point of view. A techno-economic analysis allowed to verify whether the system had the actual potential to be implemented at industrial scale. To do this, technical models were essential to simulate the functioning of the technologies in the same conditions to those in which the entire chain would be analysed. It is worth to mention that all technical models were implemented in Python.

As far as the simulation of the NF unit was concerned, a multi-scale model, covering precisely three different scales, was employed: (i) a small-scale model, with a 1-D discretization of the NF membrane approach, that described the transport mechanisms within the NF membrane, (ii) a medium-scale model for a single NF unit and (iii) a large-scale model of a whole NF plant. The small-scale model consisted in the Donnan Steric Pore Model with Dielectric Exclusion (DSPM-DE), nowadays widely used in the scientific community. More precisely, the DSPM-DE employed the extended Nernst-Plank equation to describe the ionic transmembrane phenomena, considering: (i) convection, (ii) diffusion and (iii) electro-migration of the ions across the membrane. Meanwhile, the Hagen Poiseuille equation was used to compute the solvent flux across the NF membrane. The small-scale model was then integrated in a medium-scale model which referred to an NF element.

The length of the NF element was also discretised in a series of intervals. For each interval, average values of the ionic concentrations, flow rates and pressure were firstly guessed to calculate crucial variables (i.e., the osmotic pressure and the bulk mass transfer coefficient within the NF element). Then, the small-scale model allowed to compute the ions rejections and the solvent flux. Finally, the outlet concentrations and flow rates of each discretized interval were computed by means of mass balance equations. Finally, the large-scale model aimed at calculating the total number of vessels required to reach a specific value of recovery via an iterative approach. All in all, the NF technical model was previously presented by Micari et al. [55], validating such model for similar brine compositions and operating conditions to those of this work. For the sake of brevity, all equations of the NF technical model are reported in Appendix A.

As for the MRC unit, no existing model had been yet developed. As previously mentioned, the MRC is based on two consecutive precipitation steps: (i) the precipitation of $Mg(OH)_2$ and (ii) the precipitation of $Ca(OH)_2$. More specifically, to the best of the authors' knowledge, kinetics concerning the chemical precipitation of $Mg(OH)_2$ are still not available in literature. For this reason, a simplified process model was employed, taking into account (i) mass balance equations and (ii) an instantaneous reaction between magnesium (present in the feed stream) and hydroxyl ions (present in the alkaline stream). Mass balance equations allowed to estimate the NaOH flow rate to reach pH values equal to 10.4 and 13 for $Mg(OH)_2$ precipitation and $Ca(OH)_2$ precipitation, respectively. Such equations also took into account typical conversion factors of magnesium and calcium into their respective hydroxides, based on experimental data provided in [46]. Furthermore, the required flow rate of HCl for neutralization purposes of the MRC effluent was estimated. As for the precise geometry of the MRC unit considered for the techno-economic analysis, this was the same as that of the pilot-scaled magnesium crystallizer previously developed by Vassallo et al. [46]. See Appendix A for all equations of the MRC technical model.

On the contrary, a detailed mathematical model, previously presented by Micari et al. [53], was used to simulate the MED unit. A Forward Feed configuration was taken into account in which both feed and vapour flowed in the same direction. Generally, for each effect of the MED unit, mass flow rates, temperature and pressure profiles were computed via mass and energy balance equations. However, the MED model comprised three different classes of effects for which different mass and energy equations were applied: (i) the first effect, (ii) the intermediate effects and (iii) the last effect with the end condenser. For the sake of brevity, all equations can be consulted in Appendix A. Among the three classes of effects, the first one was the only one which received heat from an external source and where the feed stream had been through all the preheaters. The feed of the first effect was sprayed onto a tube bundle whereas the heat from the external source circulated within the tubes. Vapour, generated by the partial evaporation of the feed stream, then crossed the demister and the first preheater, where it partially condensed. The part that did not condense was fed to the next effect where it acted as the heating source. The remaining brine that exited the first effect was also fed to the next effect where it was sprayed on the external surface of the tube bundle. As already mentioned, the modelling of the intermediate effects was slightly different. It comprised two energy balances on the preheater and on the heat exchanger, required to calculate the condensed fraction on the preheater tube surface and evaporated fraction of the feed stream, respectively. As for the modelling of the last effect, the latter did not have any preheater and all the vapour was sent directly to the end condenser, where it condensed completely. This was mathematically translated into different energy balances on the effect and on the last flashing box, since the total vapour in the last effect condensed in the end condenser and then collected in the flash box. The brine that exited the last effect was the final brine of the entire MED plant meanwhile the condensate of the flash box was the final distillate of the plant. Such outlets however had to respect the global mass balance equations. As far as the end condenser was

Table 3
Main inputs and outputs of the technical model of each unit in the MLD system.

Technology	Main input parameters (technical model)	Main outputs (technical model)
Nanofiltration (NF)	• Inlet flow rate [m³/d] • Inlet ions concentrations [g/L] • Membrane ions rejections [−] • Operating pressure [bar] • Permeate recovery [%] • Number of elements (vessel) [−]	• NF retentate flow rate [m³/d] • NF permeate flow rate [m³/d] • Retentate ions concentrations [g/L] • Permeate ions concentrations [g/L] • Number of vessels in parallel [−] • Electricity demand [kWh$_{el}$]
Magnesium Reactive Crystallizer (MRC)	• Inlet flow rate [m³/d] • Inlet ions concentrations [g/L] • NaOH concentration (1st/2nd stage) [g/L] • Mg conversion factor 1st stage [%] • Ca conversion factor 2nd stage [%]	• Flow rate of produced hydroxides [kg/d] • Flow rate of alkaline solution [m³/d] • Effluent flow rate [m³/d] • Outlet effluent ions concentrations [g/L] • Electricity demand [kWh$_{el}$]
Multi-Effect Distillation (MED)	• Inlet flow rate [m³/d] • Inlet NaCl concentration [g/L] • Steam Temperature [°C] • Outlet NaCl concentration [g/L] • Number of effects [−]	• Distillate flow rate [m³/d] • Outlet brine flow rate [m³/d] • Outlet brine ions concentration [g/L] • Area of heat exchangers [m²] • Heat demand [kWh$_{th}$] • Electricity demand [kWh$_{el}$]
NaCl Thermal Crystallizer (NTC)	• Inlet flow rate [m³/d] • Inlet ions concentrations [g/L] • Inlet feed temperature [°C] • Operating temperature [°C] • NF membrane rejection correction factor [−] • Total NaCl recovery (MED + NaCl Cryst) [%]	• Distillate flow rate [m³/d] • Outlet effluent flow rate [m³/d] • Outlet effluent ions concentration [g/L] • Outlet flow rate of NaCl produced [kg/d] • Purity of NaCl produced [%] • Heat demand [kWh$_{th}$] • Electricity demand [kWh$_{el}$]

concerned its feed was used to condensate the vapour. The required total cooling water flow rate was computed by means of the heat balance and the surplus was cooled down and reused.

Finally, a simplified process model for the NTC was developed, based on (i) mass and (ii) enthalpy balance equations (see Appendix A). Given as an input a desired value of global NaCl recovery from the "evaporative technologies" (MED + NTC), mass balance equations allowed to compute the mass flow rates of NaCl, brine and distillate. Meanwhile, simple enthalpy balance equations enabled to estimate the quantity of thermal energy required for evaporation, taking into consideration the sensible and latent heat and the operating temperatures of the crystallizer. Furthermore, in order to assess the purity of NaCl produced, logical conditions were integrated within the equations of the technical model. These conditions took into account the precipitation of different by-products that could compromise the final purity of NaCl produced according to the desired value of NaCl recovery and operating parameters (i.e. operating temperature). The introduction of such logical conditions was made possible thanks to a set of data achieved with PHREEQC software. More precisely, given the ionic composition of the NTC feed at a specific pressure and temperature as inputs to PHREEQC software, it was possible to identify the compounds that typically precipitate at those operating conditions, returning their solubility by means of the

thermodynamic Pitzer model. Results of the PHREEQC simulations allowed therefore to introduce logical conditions within the model to take into account the precipitation of by-products which influenced the purity of NaCl produced.

All in all, a global insight of technical models is given in Table 3 which reports the input parameters and the main outputs for each technical model:

4. Economic models

In order to evaluate the economics of each technology, each process model was coupled to an economic one. More precisely, the main outputs of each technical model became the inputs for the respective economic model. Like the technical models, also the economic models were implemented in Python.

Concerning the NF unit, the economic model followed the Verberne cost model [56] in which all equations were based on practical data provided by NF units suppliers [56]. More specifically, the capital costs were given by four different contributions: (i) the cost for buildings housing the plant, (ii) the cost for pumps, filters and piping, (iii) the cost for the energy supply systems and (iv) the investment for the membrane modules. Each capEX contribution was updated using the chemical engineering price index *CEPCI* (referred to year 2021). Furthermore, all capEX contributions were depreciated considering a specific depreciation period (30 years for buildings, 15 years for piping, pumps and energy systems and 5 years for the membrane modules). A discount rate i of 6 % was considered as it is a typical value for desalination plants [57]. As for the operating costs of an NF plant, the costs of electrical energy consumption, chemical consumption, maintenance, quality control and daily operation were considered with a plant availability equal to 8000 working hours per year. The last three contributions were estimated to be 2 % of the total capEX of the NF unit. For the sake of brevity, equations of the NF economic model are reported in Appendix B.

It is worth mentioning that the economic models of the MRC, MED and NTC units followed the Bare Module Cost Technique for the estimation of capital costs [58]. Generally, such technique is widely employed in literature as a standard tool for economic assessments of chemical plants [58]. According to this technique, capital costs were functions of the purchased cost of equipment. The purchase cost of equipment in standard conditions C_p^0 [€] (i.e. operating at ambient pressure and fabricated from the most common material, usually carbon steel) was estimated. The C_p^0 values were functions of the actual size of the equipment. Such values were then actualized using the CEPCI index and updated by a global correction factor F_{BM} to take into account direct costs (equipment, materials and labour), indirect costs (freight, overhead and engineering) and non-standard conditions concerning operating pressure and materials. The achieved values C_{BM} [€] were summed and further updated by two correction factors to account contingency and fee ($\alpha_{cont} = 15$ % and $\alpha_{fee} = 5$ % of the total C_{BM}, respectively). Finally, the total module cost C_{TM} [€] was depreciated within a period of 20 years with a discount rate i of 6 %. See Appendix B for capEX of the MRC, MED and NTC.

As far as the operating costs of the MRC were concerned, these included (i) the cost of energy consumption for pumping and the drum filter, (ii) the cost of reaction chemicals (NaOH solution for the first and second stage) and (iii) the cost of chemicals for the neutralization step (HCl solution to restore the pH of the final brine). The operating costs of the MED unit included (i) the electric energy consumption, (ii) the thermal energy consumption and (iii) the chemical consumption for cleaning, anti-scaling and anti-foaming purposes. Finally, operating costs of the NTC unit took into account (i) the cost of electric energy consumption for pumping, (ii) the cost of thermal energy required for the precipitation of NaCl crystals and (iii) the disposal cost of the final brine. Furthermore, the least expensive conventional brine treatment method was integrated in the operating costs of the NTC: Surface water discharge (0.2905 €/m³ of brine). See Appendix B for the opEX of the

Table 4

Specific costs of chemicals and energetic sources employed in the economic analysis.

	Specific cost*	
Mg(OH)$_2$	1000	€/ton [59,60]
Ca(OH)$_2$	125	€/ton [61]
Water	0.83	€/m^3 [59]
NaOH	330	€/ton [62]
HCl	125	€/ton [63]
NaCl	66	€/ton [64]
Electricity	0.2	€/kWh **
Waste heat	0.0083	€/kWh*** [53]

* All specific costs expressed in $ in the quoted references were converted in € considering a currency conversion factor (April 2021) equal to 0.83€/$.

** The specific cost of electricity refers to industrial user's cost in Pantelleria, Italy.

*** The specific cost of waste heat is assumed to account also for the depreciation costs of equipment (e.g. heat exchangers) needed to valorise it.

Table 5

Set of ion rejections of the NF membrane (operating conditions: permeate recovery = 60 %; pressure = 20 bar).

	Ionic species						
	Na$^+$	Ca^{2+}	Mg^{2+}	K$^+$	Cl$^-$	SO$_4^{2-}$	HCO$_3^-$
Membrane rejection [%]	6	50	71	5	12	91	45

MRC, MED and NTC.

The economic analysis of the proposed MLD process was carried out taking into account the main specific costs of chemicals and energy sources reported in Table 4:

Such specific costs were the main inputs for the economic analysis. Moreover, for the Pantelleria case study, typical electricity and waste heat costs of the island were employed. More precisely, waste heat was used for the analysis since at the moment renewable energy still suffers from high capital costs. All operating costs were estimated considering an annual plant availability equal to 8000 working hours/year.

5. Simulation approach

In order to evaluate the global performances of the entire treatment chain, models (both technical and economic) of all technologies were interconnected in a single workflow sheet using RCE software. RCE is an innovative tool that was recently developed by the German Aerospace Centre (DLR). Thanks to its particular characteristics that are reported in

[30], RCE seemed to be the ideal tool to easily integrate multiple models and carry out the techno-economic analysis, thus reaching the authors' needs. Within RCE, each technology was represented by a block in which technical and economic models, implemented in Python, were recalled. For each technology there were external inputs. Furthermore, the process outputs of one model became the process inputs of the following model present in the chain. Between one model and another, there were further scripts based on simple mass balance equations for the mixing of multiple streams (e.g., mixing between the NF permeate and the MRC effluent). The economic feasibility of the entire chain was then evaluated by 5 main global parameters, four of which were: (i) Levelized cost of water (LCOW$_{ater}$), (ii) Levelized cost of Mg(OH)$_2$ (LCOM$_{g(OH)2}$), (iii) Levelized cost of Ca(OH)$_2$ (LCOC$_{a(OH)2}$), and (iv) Levelized cost of NaCl (LCOS$_{alt}$). In general, the Levelized Cost is the selling price of a certain product (i.e., water, salt, etc.) that reaches the break-even point after a certain plant lifetime. Assuming that the produced flow rate of a specific product and the operating costs were the same for every year in the plant lifetime, the levelized cost of the ith product could be calculated as follows:

$$LCOith = \frac{\sum_{units} capEX + \sum_{units} opEX - \left(\sum_{units} REV - (REV_{i^{th}})\right)}{Q_{ith} (or\ V_{i^{th}}) * N_{oper,hours}}$$ (1)

where the $LOCith$ was the Levelized Cost of the ith product of interest [€/ton or €/m^3 (according to the units in which the product quantity was expressed)], $capEX$ were the depreciated capital costs of each unit/technology within the treatment chain [€/year], $opEX$ were the operating costs of each unit [€/year], REV was the revenue of each technology [€/year] and Q_{ith} (or V_{ith}) was the annual quantity of the product of interest produced [ton/h or m^3/h]. The last main parameter was the Brine Treatment Specific Cost (BTSC) defined as:

$$BTSC = \frac{\sum_{units} capEX + \sum_{units} opEX}{V_{Brine\ feed} * N_{oper,hours}}$$ (2)

where the $BTSC$ was expressed in €/m^3 of brine fed and $V_{Brine\ feed}$ was the annual brine fed to the treatment chain [m^3/h].

6. Results and discussion

The analysis carried out by this work was essentially split into two parts:

(i) a technical analysis aimed at investigating the influence of certain parameters (i.e., NF membrane) on the characteristics of a
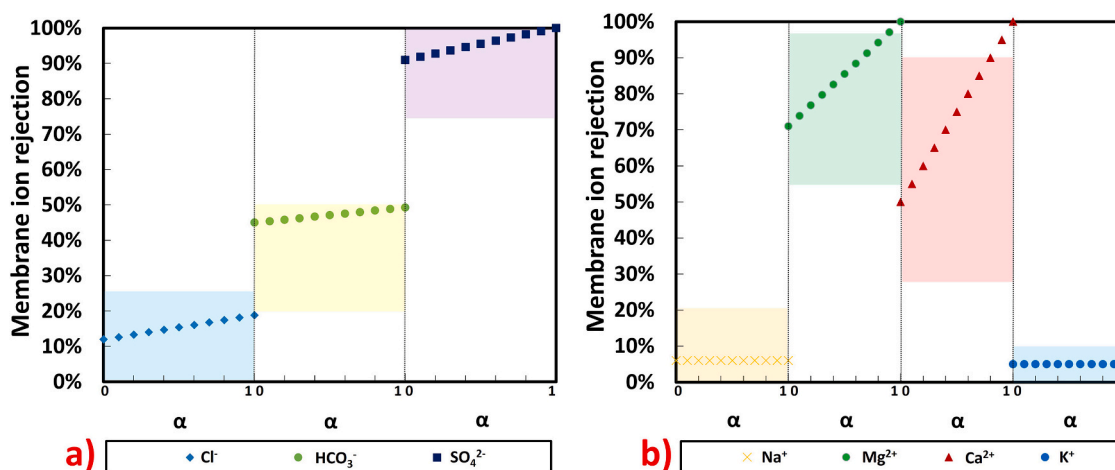

Fig. 3. a) Trend of membrane rejection of cations with α (ranging from 0 to 1); b) Trend of membrane rejection of anions with α (ranging from 0 to 1). Colored areas for each ion indicate the typical rejection values of commercial NF membranes.
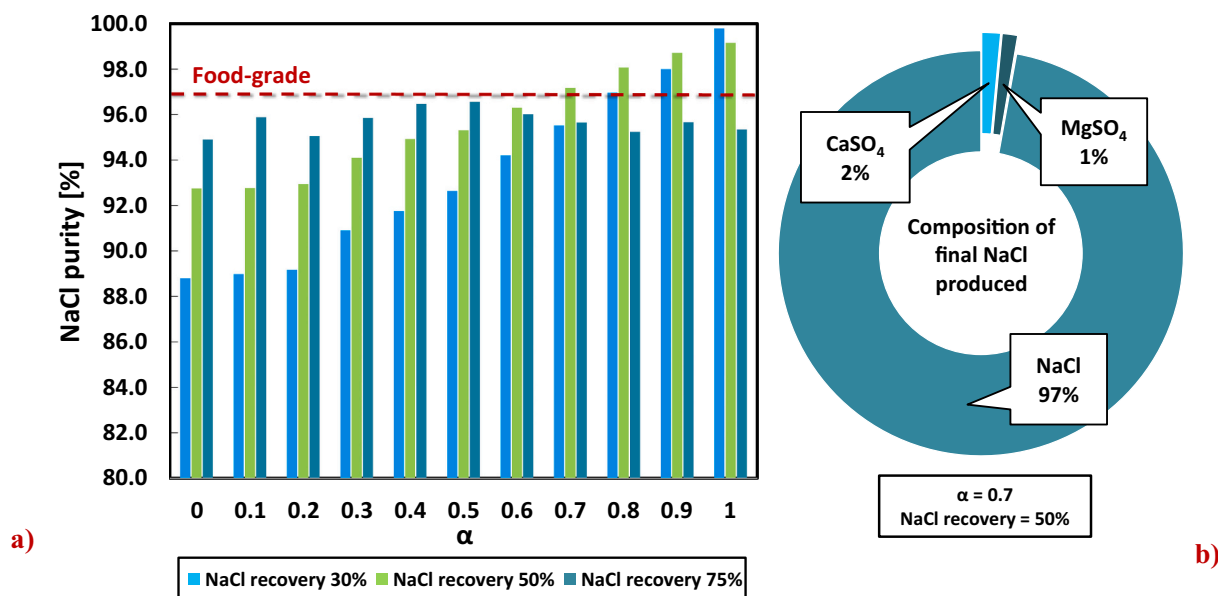
Fig. 4. a) Trend of purity of NaCl produced at different values of α and NaCl recovery; b) composition of the final NaCl produced at food-grade obtained with α = 0.7 and NaCl recovery = 50 %.

Table 6
Ionic composition and flow rates of the main streams of the MLD process.

Ion	NF feed	NF retentate	NF permeate	MED feed	MED brine	NTC brine
	Concentration [g/L]					
Na^+	21.4	20.7	20.9	21.2	107	5.90
Mg^{2+}	2.70	5.98	0.37	0.21	1.08	0.13
Ca^{2+}	0.88	1.84	0.20	0.13	0.65	0.04
K^+	0.78	0.79	0.74	0.63	3.15	0.24
Cl^-	39.0	43.9	34.3	31.4	158	6.45
SO_4^{2-}	5.50	12.9	0.24	3.18	16.0	0.02
HCO_3^-	0.18	0.19	0.08	0.05	0.25	0.02
Flow rate [m^3/d]	2280	950	1330	2330	398	135

Table 7
Flow rates of the products of the MLD process.

	Product				
	$Mg(OH)_2$	$Ca(OH)_2$	Water (MED)	NaCl	Water (NTC)
Flow rate	12,956 kg/d	2923 kg/d	1932 m^3/d	64,992 kg/d	252 m^3/d

final valuable selling product, thus evaluating the performances of the treatment chain;

(ii) an economic analysis seeking to identify the main contributors to the global economic feasibility of the chain by varying characteristics of one of the technologies (such as the number of MED effects) or different specific costs (i.e., cost of electricity).

6.1. Feasibility analysis of nanofiltration membrane rejections and NaCl recovery

For the technical analysis (and also for the economic analysis) the brine composition reported in Table 2 was considered and an inlet brine flow-rate equal to 2280 m^3/d was fixed (50 % of the total brine produced by 3 of the 4 operating RO units of Sataria desalination plant). As for the

NF plant (pre-treatment step/first step of the MLD system), spiral-wound elements were considered, each one presenting 5 membrane leaves wounded together. In analogy with a large-scale industrial plant, 6 elements were placed in series within a pressure vessel. Along each pressure vessel, the retentate of one element became the feed to the following element whereas the permeates of all elements of the same pressure vessel were mixed together. Furthermore, a number of pressure vessels was placed in parallel in order to reach a certain permeate recovery. Typical NF industrial operating conditions in the brine management field were also fixed for the case study: a permeate recovery equal to 60 % at an operating pressure of 20 bar. Last but not least, a set of membrane ion rejections was required. For such set, a thorough analysis of existing works in literature concerning NF rejections was carried out. Apart from very few exceptions, it was found that mainly the commercial membrane NF270 (Filmtec) has been employed till now to treat desalination brines. Taking into account the several set of rejections reported in literature at similar operating conditions and similar brine compositions (i.e. [65–67]), an average value for each ion was considered for this particular case study. The set of rejections is reported in Table 5:

However, as can be observed in Table 5, the membrane did not seem to be high performing in terms of calcium and magnesium membrane rejections. In fact, only 50 % of calcium was rejected, causing a severe negative impact on the remaining chain for two reasons: (i) only 50 % of calcium was recovered as calcium hydroxide (less total revenue) and (ii) 50 % of calcium that enriched the permeate was more likely to incite scaling formation within the MED unit and reduce the purity of the final NaCl product. The same was for the rejection of magnesium having an even greater influence on the global economics (since the selling price of magnesium hydroxide was much higher than that of calcium hydroxide). Aiming at food-grade salt (NaCl) quality, it was essential to reach a final purity of at least 97 % (according to the Codex Alimentarius [68]). To reach such aim, a technical analysis of the influence of NF ions rejections on the NaCl purity was performed. The theoretical analysis consisted in firstly introducing two correction factors: α and β. Rejections of ions with a similar behaviour (transport across the NF membrane) were corrected by the same correction factor [69]. Therefore, the rejections of Mg^{2+}, Ca^{2+} and SO_4^{2-} (which present also a similar dimension) were corrected by α. As for HCO_3^- and Cl^-, β was employed. Meanwhile, the rejections of Na^+ and K^+ (which are usually very low
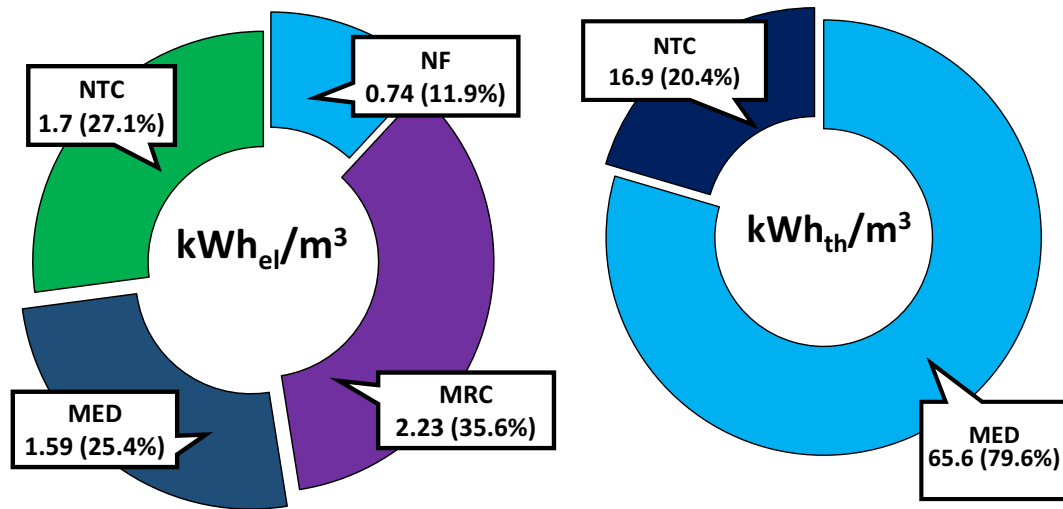
Fig. 5. Distribution of the electrical and thermal energy consumption per m³ of intake brine in the MLD system.
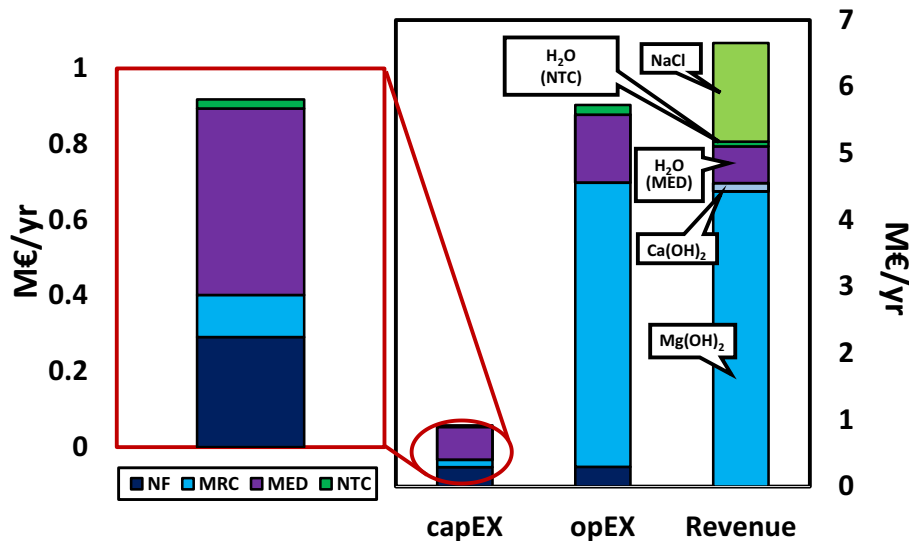

Fig. 6. Global economics of the proposed MLD system expressed in million (M) euros per year. CapEX and opEX bars refer to the 4 technologies according to the same legend shown in the inset.

and vary little at different operating conditions) were considered to be constant. Eqs. (3) and (4) describe how the bivalent and monovalent ions vary with α and β, respectively:

$$R_{ith}^{NEW} = R_{ith}^{\circ} + \alpha \bullet \left(1 - R_{ith}^{\circ}\right) \tag{3}$$

$$R_{jth}^{NEW} = R_{jth}^{\circ} + \beta \bullet \left(1 - R_{jth}^{\circ}\right) \tag{4}$$

where ith and jth refer to the generic bivalent ion (Mg^{2+}, Ca^{2+} and SO_4^{2-}) and monovalent ion (Cl^- and HCO_3^-), respectively. R° and R^{NEW} were the initial rejection value (reported in Table 5) and the updated rejection value. As already mentioned, α and β were the correction factors for the bivalent and monovalent ions, respectively.

Precisely, the analysis consisted in varying the value α within a range 0 to 1 at fixed intervals of 0.1. When α was equal to 0, $R^{NEW} = R^{\circ}$, meanwhile for α equal to 1, $R^{NEW} = 100$ %. On the other hand, for each fixed value of α, β was calculated in order to ensure electroneutrality of the solution (NF permeate and NF retentate). Results of the analysis are reported in Fig. 3(a) and (b), where the rejection of a particular ion was plotted and compared with the typical rejection values of commercial

NF membranes (coloured areas), which have been tested and employed in the past for seawater brines (i.e. [65–67]). As can be observed, values of α higher than 0.8 produced unrealistic sets of rejection with single ion rejections that were out of the so-called "real and commercial" range. Therefore, α = 0.8 was considered a critical scenario, whereas 0.7 had been assumed in all our simulations as an optimistic, yet realistic, value (since it returned a set of rejections that still lied within the typical ranges).

However, the main aim of the analysis was to identify the minimum value of the correction factor α that guaranteed a minimum NaCl purity of 97 % to be sold as a food-grade product. Therefore, PHREEQC software was used to assess the purity of NaCl produced at different NaCl recoveries. Reasons for using PHREEQC lied within its reliability demonstrated for such purposes in previous works in the past [31]. For the simulations, considering the MED and NTC as a single unit, MED inlet concentrations were required as inputs. Since the latter were given by mixing of the NF permeate and MRC, all parameters of the MRC (geometrical and operating conditions) were fixed in order to not influence whatsoever the analyses based on different values of α. In particular, typical experimental values were fixed for the concentration
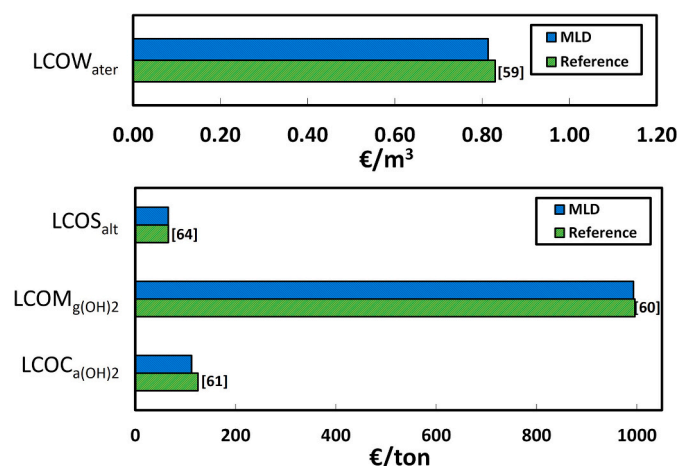
Fig. 7. Levelized costs of valuable products (LCOW$_{ater}$ = Levelized Cost of Water; LCOS$_{alt}$ = Levelized Cost of Salt; LCOM$_{g(OH)2}$ = Levelized Cost of Mg (OH)$_2$; LCOC$_{a(OH)2}$ = Levelized Cost of Ca(OH)$_2$) compared to their actual market prices.
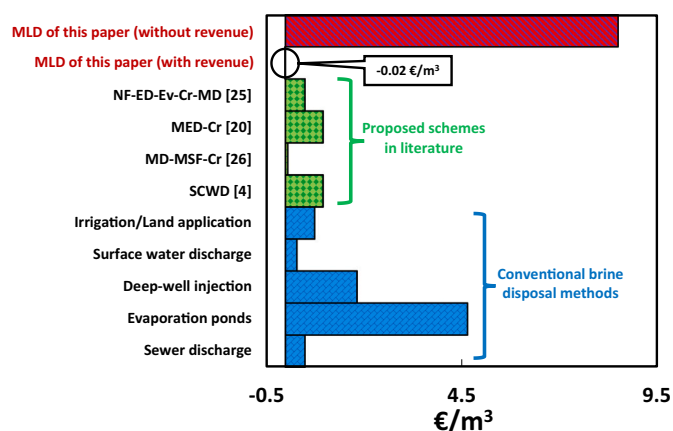

Fig. 8. Comparison between conventional methods costs [64], proposed schemes in literature and BTSC of the proposed MLD with and without accounting for the revenues.

of NaOH (1 mol/L) and for the conversion factors of Mg^{2+} (95 %) and Ca^{2+} (97 %) for the first and second stage, respectively. These conditions were not varied for further analyses. Along with the concentrations given as inputs in PHREEQC, the quantity of water (to evaporate) was fixed. It was fixed accordingly to ensure a certain recovery of NaCl. Subsequently, based on the products precipitated, the purity of NaCl produced was calculated.

As previously mentioned, for each value of α, the purity was evaluated at three different values of NaCl recovery: 30 %, 50 % and 75 %. Results are depicted in Fig. 4(a):

Results illustrated in Fig. 4a) show how purity increased with α at low recoveries (30 %) of NaCl. This was mainly due to the fact that greater quantities of magnesium and calcium were rejected by the NF membrane and subsequently recovered as hydroxides in the MRC. This, therefore, led to minor quantities that could precipitate and compromise the purity of the final selling product. A similar trend could be observed for an NaCl recovery of 50 %. However, the increase of purity in this specific case presented a reduced slope. Reason for this was that when attempting to recover more NaCl (evaporating more water), more impurities tended to precipitate. As a matter of fact, very high NaCl recoveries (75 %) did not rather lead to a net increase of purity with α but tended to fluctuate around an average value. It is also interesting to see

that this value was always lower than 97 %, therefore unsuitable for the food-grade target. The target, on the other hand, was possible to reach at an NaCl recovery of 50 % and α equal to 0.7. As mentioned earlier, 0.7 was still a value that allowed to operate within a realistic range of NF membrane ion rejections. Finally, taking into account these suitable conditions, Fig. 4b) represents the percentage of the impurities of the final NaCl product. Precisely, the main compounds that precipitated with NaCl were CaSO$_4$ and MgSO$_4$ that represented 2 % and 1 % of the total solid product, respectively.

In addition, taking into account a value of α equal to 0.7, the ionic composition and flow rates of the main streams of the MLD process are listed in Table 6. As can be observed in Table 6, only 6 % of the initial SWRO brine was discharged back to the environment, making the MLD process an "almost-ZLD" process.

Table 7, moreover, reports the flow rates of the products recovered from the MLD process.

6.2. Economic analysis

6.2.1. Analysis of the base case scenario

Once the optimal value of α (required for the achievement of 97 % purity of NaCl) was identified, a thorough economic analysis of the proposed MLD system was performed to evaluate its feasibility. It is important to highlight that the compositions and flow rates of the MLD system analysed were the ones listed in Tables 6 and 7. Until now, no specific information concerning the operating conditions of MED and NTC has been given since the previous technical analysis considered the MED unit and the thermal crystallizer as a single black box. However, for the economic analysis it was necessary to define such conditions. As far as the MED was considered, 10 effects were considered (typical industrial value) operating at a TBT of 110 °C. This temperature was possible due to the NF upstream. The NTC, on the other hand, presented 5 effects at a maximum operating temperature of 100 °C. Both the MED and NTC employed waste heat (supplied from flue gases produced in a near-by power plant). This allowed to reduce operating costs for the energy-intensive technologies of the chain. As can be observed from the techno-economic analysis results in Fig. 5, MED was one of these technologies (positioned in third place for electricity). As regards the thermal energy consumption, MED consumed more than double the amount of heat when compared to the NTC. Moreover, it is worth noting how the specific electric consumption of the MRC was the highest. This was due to the Drum filter employed for the recovery of hydroxide solids from the produced slurry.

Anyhow, energy consumption was just one of the several factors that contribute to the total cost of the treatment chain. Results of the global economics of the entire MLD system are reported in Fig. 6.

In Fig. 6 it is possible to see how capital costs were much less than the operating costs. NF and MED contributed to the majority of the capital costs: NF for its membranes and MED for its multiple effects with its several heat exchangers. As for the operating costs, it was the MRC that led to overall high operating costs. This was mainly due to the use of large amounts of expensive alkaline reactants (i.e. NaOH) followed by the use of chemicals (HCl) for the final neutralization step. As can be expected, another major contributor was the MED. However, regardless the high overall costs, the total revenue achieved was higher than the capEXs and opEXs of the MLD system. Revenues were so high thanks to the high selling price of Mg(OH)$_2$ followed by the large amounts of NaCl produced. Since the revenues were higher than the sum of capital and operating costs, the Levelized costs of the valuable products obtained from the chain were lower than their selling price. Fig. 7 illustrates all levelized costs. From Fig. 7 it is possible to observe that the levelized cost of salt (LCOS$_{alt}$) was equal to the typical market price (i.e. 66 €/ton) making the treatment chain still a competitive integrated technology for the production of salt. All other Levelized Costs were even lower than their respective market price.
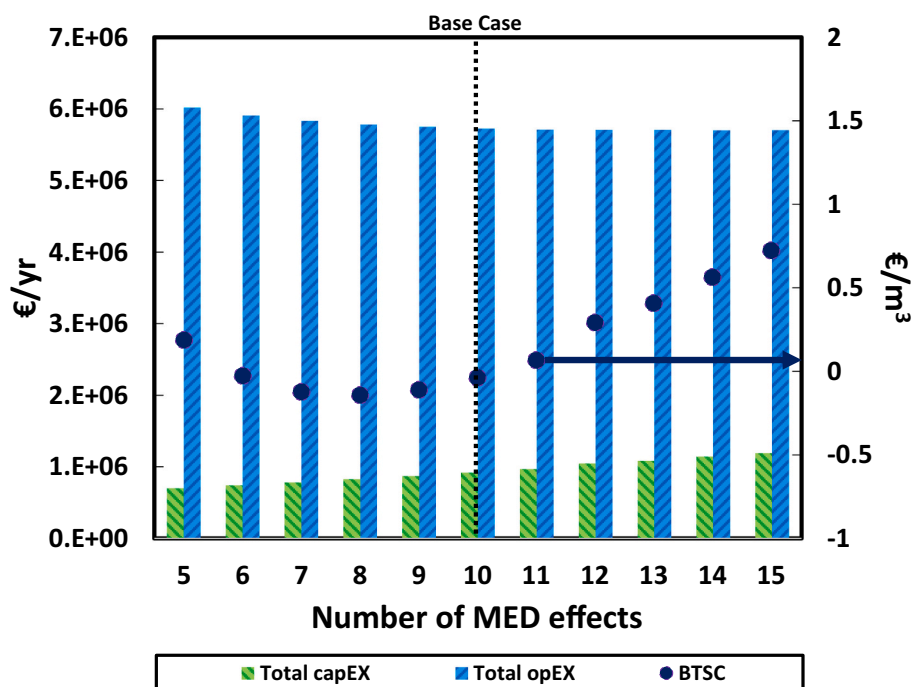
Fig. 9. Trend of total capEXs, total opEXs and BTSC factor of the entire treatment chain with the number of MED effects. The polynomial curve that links the BTSC factors at different numbers of MED effects has also been represented.

Table 8
Range of specific costs of chemicals and energetic sources employed in the parametric analysis.

	Typical range of specific cost*	
$Mg(OH)_2$	580–1162	€/ton**
$Ca(OH)_2$	42–208	€/ton [61]
Water	0.42–1.66	€/m³ [70]
NaOH	166–498	€/ton [62]
HCl	83–250	€/ton [71]
NaCl	42–125	€/ton [64]
Electricity	0.08–0.25	€/kWh [72]

* All specific costs were converted in € considering a currency conversion factor April 2021 equal to 0.83 €/$.
** Range of the specific cost of magnesium hydroxide derives from an internal economic analysis carried out by UNIPA.

6.2.2. Economic comparison with other brine disposal/treatment concepts

The economic feasibility of the entire chain was also evaluated looking at the Brine Treatment Specific Cost (BTSC, as defined in Section 5). Fig. 8 compares the brine treatment cost of the proposed MLD system with conventional brine disposal methods and new proposed brine valorisation schemes present in the literature.

Taking into account only capital and operating costs but neglecting any revenue (Fig. 8), the chain was much less attractive than the already existing brine disposal methods. More precisely, the BTSC factor was equal to 8.49 €/m³ (much higher than the 4.65 €/m³ required with evaporation ponds). However, when the sale of all the valuable products recovered by the integrated chain was taken into consideration, the brine treatment specific cost BTSC reached a value near zero, thus being much lower than that of both the conventional methods and recent proposed schemes in literature (Fig. 8). To be noted that the brine treatment cost given by the schemes present in literature (0.5 €/m³ [25], 0.96 €/m³ [20], 0.06 €/m³ [26], 0.96 €/m³ [4]) already take into account the sale of the valuable goods that they produce. In particular, the BTSC of the treatment chain proposed here (=−0.02 €/m³) assumed a negative value, due to the fact that the sum of capEXs and opEXs of the treatment chain was lower than the overall revenue achieved. Having a

negative BTSC factor unlike the conventional and new brine disposal costs could be translated into dealing with an admirable market-competitive technology where brine treatment is no longer a cost and a net saving is achieved. Of course, such outcomes must be considered as reliable only by referring to the current market conditions for any of the products considered: a possibility that such conditions change as soon as the proposed chain is implemented at large scale may exist.

6.2.3. Influence of the MED number of effects on the economic performance of the MLD scheme

The overall techno-economic analysis had shown and demonstrated the economic feasibility of the MLD system, applied as a hybrid technology to promote brine volume minimization, mineral recovery and water production. However, results of such analysis were referred to a treatment chain, which comprised an MED unit with a precise technical design (i.e. 10 effects). Therefore, it was interesting to investigate how the total costs and the BTSC factor could change by varying the number of MED effects. Fig. 9 shows the trend of total capEXs, total opEXs and the BTSC factor of the treatment chain with the number of effects. Considering a range of effects between 5 and 15, it is worth noting how capEXs and opEXs presented opposite trends when the number of MED effects increased leading to an overall minimum value of the BTSC factor equal to −0.14 €/m³ (precisely when 8 effects were reached). Capital costs augmented mainly due to the increase of units (which meant more heat exchangers, more condensers etc.) whilst operating costs primarily decreased due to the reduction of thermal energy consumption required by the MED. Meanwhile the increase of operating costs prevailed at low numbers of effects, the increase of capital costs prevailed at higher numbers of effects, thus justifying the presence of a minimum value of the BTSC factor.

Furthermore, it is interesting to note how the minimum value of the BTSC factor was negative. The reason for such value was due to the fact that the sum of total capEXs and opEXs was lower than the total revenue obtained from the sale of all valuable goods produced.
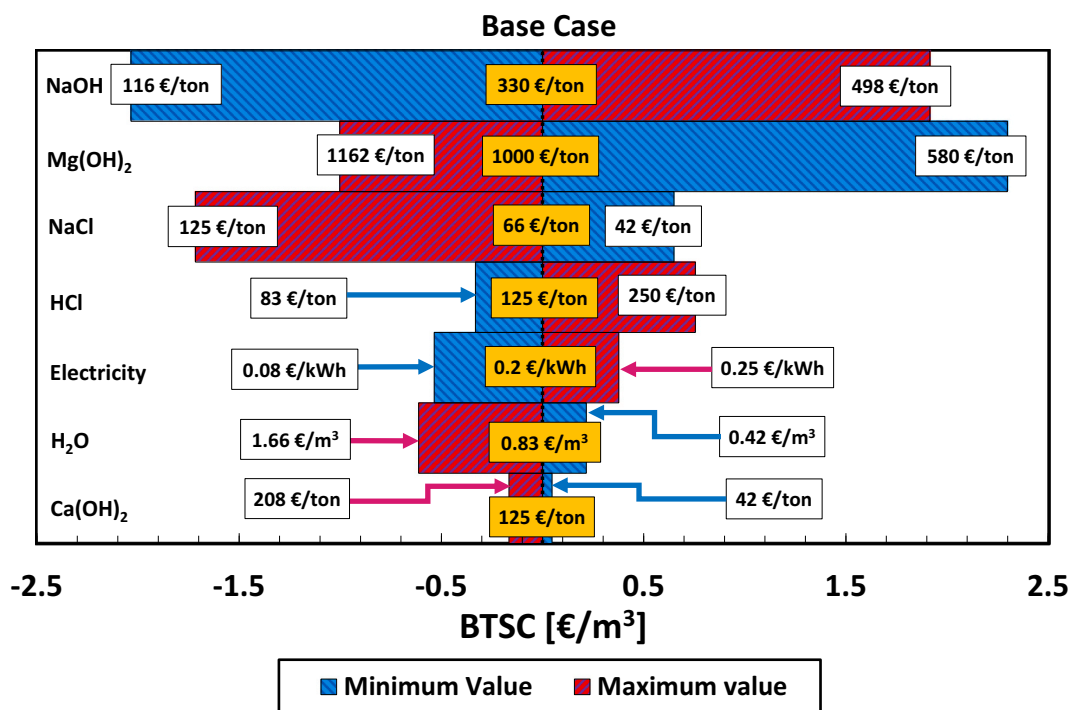
Base Case

Fig. 10. Trend of the BTSC factor at minimum and maximum commercial values of different chemical compounds and electricity. The specific costs in the white boxes are the minimum and maximum values of the ranges whereas those in the yellow boxes are referred to the base case.
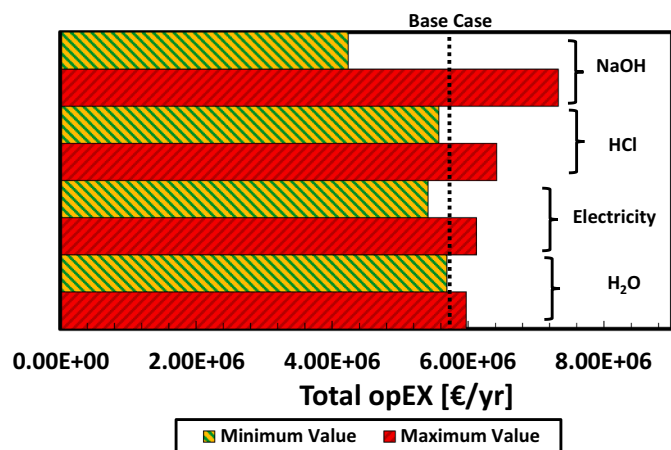

Fig. 11. Trend of the opEXs of the entire treatment chain at minimum and maximum commercial values of different chemical compounds and electricity.

6.2.4. Parametric analysis and Tornado diagram of the main factors affecting the BTSC

Once an optimal design of the MED technology was identified, a final parametric economic analysis was performed to examine the influence of specific costs of chemicals or electricity on the global economics of the proposed MLD system, with the specific costs varying within a reasonable range. Table 8 reports the typical ranges, considered for the parametric analysis, within which the cost of a specific chemical or electricity can vary. It is to be noted that the minimum and maximum value of each range correspond to those reached within year 2021 in the world.

Fig. 10 illustrates the variation of BTSC as a function of the above mentioned parametric costs, in the form of a Tornado diagram [73], highlighting the maximum and minimum value reached by BTSC when the cost of a specific chemical or electricity reached its minimum or maximum. It is worth noting that increasing the selling price of

recovered products (i.e. $Mg(OH)_2$, NaCl, $Ca(OH)_2$ and H_2O) tended to reduce the BTSC factor, since they increased the overall revenue of the treatment chain. On the other hand, NaOH, HCl and electricity increased the operating costs when their specific cost increased. Another interesting fact to observe is the larger influence of the cost variation of NaOH, $Mg(OH)_2$ and NaCl on the BTSC factor than that caused by the other contributions. More precisely, when the required NaOH was bought at a very high price (i.e. 498 €/ton) or $Mg(OH)_2$ or even NaCl were sold at their lowest prices (i.e. 580 €/ton and 42 €/ton, respectively), the BTSC factor could overcome the conventional brine treatments costs making the proposed MLD system not competitive. Such issue was not to be feared when electricity reached its highest value or $Ca(OH)_2$ and H_2O were sold at their lowest prices.

The greater influence of NaOH on the global economics of the treatment chain, compared to that of the other chemicals, is more visible in Fig. 11. More precisely, Fig. 11 proves that the largest variation of operating costs was obtained when the cost of NaOH varied between a reasonable minimum and maximum value. Variations of the cost of H_2O, on the other hand, translated into very little alterations of the operating costs from the base case value.

All in all, results of Fig. 10 and Fig. 11 demonstrate that the Magnesium Reactive Crystallizer was the technology that influenced the most the global economics of the proposed MLD system. In particular, it was the cost of the alkaline reactant (NaOH) and the price at which Magnesium Hydroxide was sold that were the driving forces of the economic feasibility of the MLD process. Large ranges of the NaOH costs and/or $Mg(OH)_2$ selling prices made the chain economically feasible. Only in extreme conditions (i.e., very high NaOH costs and very low Mg $(OH)_2$ selling prices), such feasibility was not achieved. All in all, if these extreme conditions are not reached, then the proposed treatment chain could be an attractive alternative anyway for seawater brine management.

Tornado diagram sensitivity analysis allows to evaluate the effect of a single cost item on the BTSC, meanwhile all the others are kept constant. This kind of analysis does not include any concomitant effect of more than one cost item. Thus, two additional economic scenarios are
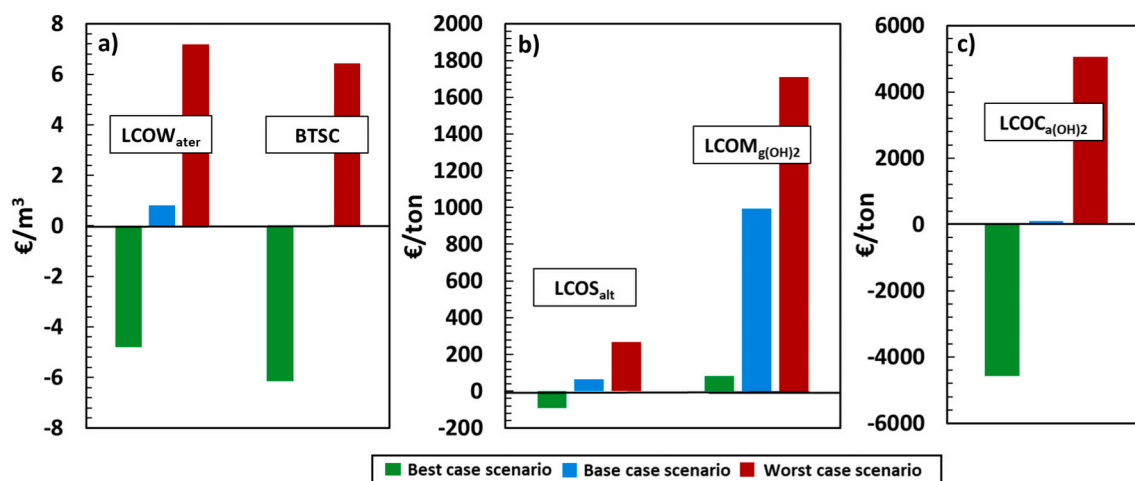
Fig. 12. Comparison between best case, base case and worst case scenario for a) Levelized cost of water and BTSC, b) Levelized cost of salt and magnesium hydroxide and c) Levelized cost of calcium hydroxide.

investigated: more precisely, it was also decided to investigate how the levelized costs of products and the BTSC factor could vary if all costs were brought to their highest value and all product selling prices were brought to their lowest values contemporarily (worst case scenario) and vice versa (best case scenario). A comparison of such scenarios is reported in Fig. 12a), b) and c). As it can be seen in Fig. 12b), the best case scenario was characterized by an extremely low $LCOM_{g(OH)2}$ (92 €/ton) whereas all the other levelized costs and the BTSC factor presented negative values (see Fig. 12a), b) and c)), making the treatment chain a very competitive technology for magnesium hydroxide production when compared to the relevant current market. On the contrary, the worst case scenario led to very high levelized costs making the proposed treatment not at all feasible from an economic point of view. This was mainly due to the fact that the total revenue could not even compensate the total sum of capital and operating costs of the MLD chain. All in all, as for the base case scenario and the best case scenario, brine disposal is no longer a costly issue. As a matter of fact, a net saving is reached: an achievement that is not at all possible with the conventional disposal methods, not even with the recently proposed schemes in literature (Section 6.2.2). As far as the worst case scenario is considered, the BTSC reached a value equal to 6.4 €/m³, a value higher than the most costly conventional brine treatment methods (4.65 €/m³). However, it is to be noted that such case is somewhat rare due to the contemporary low selling prices of all products and high costs of all required chemicals and electricity.

7. Conclusions

In recent years, literature has been reporting several treatment chains aimed at eliminating the environmental problem of brine disposal and recovering valuable minerals, contemporarily. However, most of these proposed technologies, called Zero Liquid Discharge (ZLD) or Minimal Liquid Discharge (MLD) depending on the brine volume reduction factor, suffer from high capital costs and energy consumption. This paper aimed at identifying how some of the best operating technologies at the moment available, can be effectively combined and operated in a novel and practical scheme that can reach the MLD target. The proposed chain was composed of an NF, an MRC, an MED and an NTC recovering magnesium hydroxide, calcium hydroxide, water and sodium chloride. By recovering such minerals, it was possible to reduce the volume of the final effluent at the same time. The treatment chain was proposed for a specific case study: the treatment of SWRO brines in the island of Pantelleria, Italy.

Results of the technical analysis showed that choosing a suitable set of NF rejections (still lying within the range of those of current

commercial NF membranes) it was possible to achieve food-grade NaCl in the final crystalliser.

The economic analysis of the base case scenario showed that the chain was dominated by opEXs higher (about five times) than capEXs. This was mainly due to the expensive chemicals required in the magnesium crystalliser. However, overall revenue was higher than the sum of capEXs and opEXs of the entire chain, mainly due to the sale of magnesium hydroxide produced. Moreover, the economic feasibility of the novel MLD system (as an alternative technology for the production of a specific salt) was demonstrated via the use of the Levelized Cost Index. The Levelized Cost for all products was computed and all achieved values were lower or equal to their current market prices, proving the economic sustainability of the treatment chain. A further investigation concerning the influence of the number of MED effects on the global economics identified a minimum value of the Brine Treatment Specific Cost (BTSC) equal to −0.14 €/m³ at 8 MED effects. It was additionally demonstrated that only large variations of NaOH and Mg (OH)₂ costs could significantly compromise the economic feasibility of the proposed MLD system, making the MRC technology the bottleneck of the treatment chain.

Finally, for the case of the base case scenario, the economic viability of the proposed MLD scheme was compared with (i) conventional brine disposal methods and (ii) recently proposed innovative treatment chains. Results indicate that, at the current market conditions, the BTSC relevant to the proposed scheme is lower than all the other available alternatives. As a future outlook, the proposed treatment chain may benefit from the addition of an EDBM unit downstream the MRC to produce in situ the chemicals needed for the Mg recovery [74].

CRediT authorship contribution statement

C. Morgante: Methodology, Software, Formal analysis, Data curation, Investigation, Writing – original draft, Visualization. **F. Vassallo:** Methodology, Software, Formal analysis, Data curation, Investigation, Writing – review & editing, Visualization. **D. Xevgenos:** Writing – review & editing, Supervision, Project administration, Funding acquisition. **A. Cipollina:** Conceptualization, Methodology, Validation, Resources, Writing – review & editing, Supervision, Project administration, Funding acquisition. **M. Micari:** Methodology, Software, Formal analysis, Investigation, Writing – review & editing, Visualization. **A. Tamburini:** Conceptualization, Methodology, Validation, Resources, Writing – review & editing, Supervision, Project administration, Funding acquisition. **G. Micale:** Conceptualization, Methodology, Resources, Writing – review & editing, Supervision, Project administration, Funding acquisition.

Declaration of competing interest

The authors declare that they have no known competing financial interests or personal relationships that could have appeared to influence the work reported in this paper.

Acknowledgements

Appendix A. Technical models

A.1. Nanofiltration NF technical model

The NF technical model is a multi-scale model which comprises: (i) a low-scale model that describes the transport mechanisms within the NF membrane, (ii) a middle-scale model for a single NF unit and (iii) a high-scale model of a whole NF plant.

A.1.1. Small-scale model (NF membrane)

The Donnan Steric Pore Model with Dielectric Exclusion (DSPM-DE) is employed to describe the transport mechanisms that occur within the NF membrane. Such model exploits the extended Nernst-Plank equation across the membrane. Within the equation, three different ionic transport mechanisms are considered: (i) convection, (ii) diffusion and (iii) electro-migration (see Table A1). The width of the membrane is discretized in a specific number of elements (50 based on sensitivity analyses). The 'j' index refers to the discretised element, while the 'i' index refers to a specific ion.

The main equations of the technical model are listed in Table A1, where $C_{i,j}^m$, C_i^{bm}, C_i^b and C_i^p are the concentration of the i species in the jth element in the membrane, at the bulk-membrane interface, in the bulk solution and in the permeate stream, respectively. J_i and J_v represent the total flux of the species i and the water convective transmembrane flux, respectively. ψ is the electric potential across the membrane, ξ the electric potential gradient at the bulk-membrane interface, outside the electric double layer, and $\Delta\psi_{D,bm}$ and $\Delta\psi_{D,pm}$ represent the Donnan potential difference at the bulk-membrane interface and at the permeate-membrane interface, respectively. $K_{i,c}$ and $k_{i,d}$ represent the hindered convective and diffusive mass transfer coefficients of the ions within the pore, depending on λ_i, i.e. the ratio between the solute radius (r_i) and the pore radius (r_{pore}). $D_{i,p}$ is the diffusivity of the species i within the pore, corrected taking into account the diffusivity in the bulk via $k_{i,d}$.

Ion partitioning at the two membrane interfaces, the steric effect and the dielectric exclusion are given by solving the system of equations listed in Table A1. Furthermore, contemporarily conditions which must be satisfied are the electro-neutrality on the bulk, on the permeate side and inside the membrane (which presents a fixed charge density X_d). Mass transfer resistance on the bulk side is considered to compute the ions concentration on the bulk-membrane interface. It is then possible to calculate the solute flux from the bulk to the membrane. As for the mass transfer coefficients, the mass transfer coefficient in the bulk, $k_{c,i}^{bulk}$ depends on the flow regime whereas $k_{c,i}^{'bulk}$ is obtained multiplying the mass transfer coefficient $k_{c,i}^{bulk}$ by a factor depending on the permeation flux through the membrane. The Hagen-Poiseuille relation is employed to calculate the solvent transmembrane flux J_v. Such flux depends on the geometric parameters of the membrane and on the net driving pressure, ΔP (given by the pressure gradient between bulk and permeate channel minus the osmotic pressure $\Delta\Pi$) where η_{mix} is the mixing efficiency of the spacer, h_f is the height of the feed channel, L_{mix} is the mixing length of the spacer, Pe and Sc are the Peclet and the Schmidt adimensional numbers respectively. The system of equations is implemented in Python and solved in an iterative manner.

Table A1
Equations of the implemented DSPM-DE model.

(1)	$j_i = J_v C_{i,p} = -D_{i,p}\dfrac{C_{i,j+1}^m - C_{i,j}^m}{\delta y_j} - \dfrac{1}{2}z_i\left(C_{i,j+1}^m + C_{i,j}^m\right)D_{i,p}\dfrac{F}{RT}\dfrac{\psi_{j+1} - \psi_j}{\delta y_j} + \dfrac{1}{2}k_{i,c}\left(C_{i,j+1}^m + C_{i,j}^m\right)J_v$
(2)	$k_{i,d} = \dfrac{1 + \frac{9}{8}\,\lambda_i\,ln(\lambda_i) - 1.56034\,\lambda_i + 0.528155\,\lambda_i{}^2 + 1.91521\,\lambda_i{}^3 - 2.81903\,\lambda_i{}^4 + 0.270788\,\lambda_i{}^5 + 1.10115\,\lambda_i{}^6 - 0.435933\,\lambda_i{}^7}{\phi_i}$
(3)	$k_{i,c} = \dfrac{1 + 3.867\,\lambda_i - 1.907\,\lambda_i{}^2 - 0.834\,\lambda_i{}^3}{1 + 1.867\,\lambda_i - 0.741\,\lambda_i{}^2}$
(4)	$D_{i,\,p} = k_{i,\,d}D_{i,\,\infty}$
(5)	$\dfrac{\gamma_{i,1}^m C_{i,1}^m}{\gamma_i^{bm} C_i^{bm}} = \phi_i\phi_{B_i}exp\left(-\dfrac{z_i F}{RT}\Delta\psi_{D,bm}\right)$
(6)	$\dfrac{\gamma_{i,N}^m C_{i,N}^m}{\gamma_i^p C_1^p} = \phi_i\phi_{B_i}exp\left(-\dfrac{z_i F}{RT}\Delta\psi_{D,pm}\right)$
(7)	$log\gamma_i = -A\,z_i{}^2\left(\dfrac{\sqrt{I}}{1 + \sqrt{I}} - 0.3\,I\right)$
(8)	$A = \dfrac{e_0{}^3\,N_A{}^{1/2}}{ln(10)\,4\pi\,\sqrt{2}\,(\varepsilon\,k_B T)^{3/2}}$
(9)	$\phi_{B_i} = exp\left(-\dfrac{\Delta W_i}{k_B T}\right)$
(10)	$\Delta W_i = \dfrac{z_i{}^2 e_0{}^2}{8\pi\varepsilon_0 r_i}\left(\dfrac{1}{\varepsilon_{pore}} - \dfrac{1}{\varepsilon_{bulk}}\right)$
(11)	$\phi_i = (1 - \lambda_i)^2$
(12)	$\sum_i z_i C_i^{bm} = 0$
(13)	$\sum_i z_i C_i^p = 0$
(14)	$\sum_i z_i C_{i,j}^m + X_d = 0$
(15)	$j_i = -k_{c,i}^{'bulk}\left(C_i^{bm} - C_i^b\right) + J_v C_i^{bm} - z_i C_i^{bm} D_{i,\infty}\dfrac{F}{RT}\xi$
(16)	

Table A1 (*continued*)

(17)	$k'^{bulk}_{c,i} = k^{bulk}_{c,i} \Xi = k^{bulk}_{c,i} \left[\dfrac{J_v}{k^{bulk}_{c,i}} + \left(1 + 0.26 \left(\dfrac{J_v}{k^{bulk}_{c,i}} \right)^{1.4} \right)^{-1.7} \right]$
	$k^{bulk}_{c,i} = 0.753 \left(\dfrac{\eta_{mix}}{2 - \eta_{mix}} \right)^{1/2} \left(\dfrac{D_{i,\infty}}{h_f} \right) Sc^{-1/6} \left(\dfrac{Pe_i h_f}{L_{mix}} \right)^{1/2}$
(18)	$J_v = \dfrac{\Delta P\, r_{pore}^2}{8\, \eta\, \delta_m}$
(19)	$\Delta\Pi = RT \sum_i \left(C^{bm}_i - C^p_i \right)$

A.1.2. Medium-scale model (NF element)

The medium-scale model refers to an NF element in which the low-scale model is integrated. The length of the NF element is discretised in a series of elements. For each element, average values of the concentration, flow rates and pressure are firstly guessed to calculate the osmotic pressure and the bulk mass transfer coefficient. Then, the small-scale model allows to compute the ions rejection and the water flux. Finally, the outlet concentrations and flow rates of each discretized element are computed by means of mass balances (Table A2).

Table A2
Equations to model a nanofiltration element.

$M_{p_x} = M_{p_{x-1}} + J_{vx} \dfrac{A_{membr,elem}}{n_{discr,L}}$
$M_{ret_x} = M_{bx} - J_{vx} \dfrac{A_{membr,elem}}{n_{discr,L}}$
$C^p_{ix} = \dfrac{C^p_{ix-1} M_{p_{x-1}} + j_{ix} \dfrac{A_{membr,elem}}{n_{discr,L}}}{M_{p_x}}$
$C^{ret}_{ix} = \dfrac{C^b_{ix} M_{bx} - j_{ix} \dfrac{A_{membr,elem}}{n_{discr,L}}}{M_{ret_x}}$
$M_{bx} = M_{retx-1}$
$C^b_{ix} = C^{ret}_{ix-1}$
$P_x = P_{x-1} - \Delta P_{losses} = P_{x-1} - \dfrac{f}{2} \dfrac{1}{D_H} \varrho_f u_f^2$
$f = \dfrac{6.23}{Re^{0.3}}$

M_p and C^p_i are the mass flow rate and the concentrations in the permeate channel, M_{ret} and C^{ret}_i are the flow rate and the concentrations in the retentate channel, which are the same as those entering the next interval (M_b and C^b_i), and $A_{membr,elem}$ and $n_{discr,L}$ are the total membrane area of a NF element and the number of discretization intervals along the main feed flow direction. As for the equation to calculate the pressure losses, f is the friction factor, l is the length of the discretization interval and D_H is the hydraulic diameter relevant to the feed channel.

A.1.3. Large-scale model (NF plant)

The main aim of the large scale model is to calculate the total number of vessels necessary to reach a specific value of recovery. Firstly, an initial number of vessels in parallel is given by dividing the required permeate flow rate and a guessed average solvent transmembrane flux. Then, the feed flow rate for each vessel is calculated. Subsequently, the average solvent flux in the vessel is recalculated in relation to the net driving pressure along the elements, and the total recovery rate is computed. Once such value has been calculated, the number of pressure vessels in parallel can be updated considering a linear relationship between the number of vessels and the recovery. From this point, another iteration begins. Once the value of the total recovery is higher or equal to the required one, the iteration is brought to an end.

A.2. Magnesium Reactive Crystallizer MRC technical model

The Magnesium Reactive Crystallizer MRC technical model is based on simple mass balance equations which are listed in Table B1. The MRC consists of two precipitation steps. In the first step, magnesium is recovered from the brine in the form of magnesium hydroxide $Mg(OH)_2$ by employing an alkaline reactant: a sodium hydroxide solution NaOH. In order to promote $Mg(OH)_2$ precipitation, one magnesium ion of the brine has to react with two hydroxyl ions of the alkaline solution. The mass flow rate $Q_{NaOH_{1°step}}$ of the required alkaline solution is calculated taking into account (i) such proportion with the molar flow rate of magnesium $Q_{feed,Mg^{2+}_{1°step}}$ multiplied by the effective conversion rate of magnesium $\%_{Mg^{2+}_{1°step}}$ and (ii) the quantity of NaOH which is used in precipitating the bicarbonates present in the brine where $Q_{feed_{1°step}}$ is the volumetric feed flow rate and $C_{feed,HCO_3^-_{1°step}}$ is the molar concentration of the bicarbonates in the brine. The latter phenomenon unfortunately is inevitable and has to be considered. The flow rate $Q_{NaOH_{1°step}}$ depends on the operating molar concentration of NaOH $C_{NaOH_{1°step}}$. Simple mass balance are further employed to calculate the total outlet volumetric flow rate of the 1° precipitation step $Q_{out_{1°step}}$, the mass flow rate of $Mg(OH)_2$ produced $M_{Mg(OH)_2 1°step}$ where $MW_{Mg(OH)_2}$ is the molecular weight of $Mg(OH)_2$ and the magma density of $Mg(OH)_2$ $M_{Mg(OH)_2 1°step}$. Finally the outlet ionic molar concentrations are computed where the index i is the generic ion present in the brine (K^+, SO_4^{2-}, Cl^-) All bicarbonates are precipitated in the 1° step in the form of calcium carbonates. Such precipitation influences the final concentration of calcium in the outlet stream. The outlet of the 1° step becomes the inlet of the 2° step and mass balance equations are employed to estimate the mass flow rate of calcium hydroxide $Ca(OH)_2$ produced $M_{Ca(OH)_2 2°step}$ where $\%_{Ca^{2+}_{2°step}}$ is the effective conversion rate of calcium in the second step. As far as the NaOH employed in the 2° step, its volumetric flow rate $Q_{NaOH_{2°step}}$ takes into account three contributes: (i) the stoichiometric quantity $Q_{NaOH,\, stoic_{2°step}}$ to precipitate calcium, (ii) the quantity employed to complete magnesium precipitation $Q_{NaOH,\, Mg_{2°step}}$ and (iii) the quantity necessary to reach pH = 13 to complete calcium precipitation $Q_{NaOH,\, added_{2°step}}$ where $C_{Ca(OH)_{2sol}}$ is the $Ca(OH)_2$

solubility and $C_{NaOH_{pH=13}}$ is the molar concentration of NaOH at pH 13. Finally, the volumetric flow rate of acid HCl $Q_{HCl_{TOT}}$ is computed (necessary to neutralize the final effluent exiting the MRC $Q_{effluent}$.

Table B1
Mass balance equations of the Magnesium Reactive Crystallizer plant.

1° precipitation step	2° precipitation step
$Q_{NaOH_{1°step}} = \dfrac{2Q_{feed,Mg^{2+}_{1°step}} \bullet \%_{Mg^{2+}_{1°step}} + Q_{feed_{1°step}} \bullet C_{feed,HCO_3^-_{1°step}}}{C_{NaOH_{1°step}}}$	$Q_{feed,Ca^{2+}_{2°step}} = Q_{out_{1°step}} \bullet C_{out,Ca^{2+}_{1°step}}$
$Q_{out_{1°step}} = Q_{NaOH_{1°step}} + Q_{feed_{1°step}}$	$Q_{NaOH,stoic_{2°step}} = \dfrac{2Q_{feed,Ca^{2+}_{2°step}} \bullet \%_{Ca^{2+}_{2°step}}}{C_{NaOH_{2°step}}}$
$M_{Mg(OH)_2 1°step} = Q_{feed,Mg^{2+}_{1°step}} \bullet \%_{Mg^{2+}_{1°step}} \bullet MW_{Mg(OH)_2}$	$Q_{NaOH,Mg_{2°step}} = \dfrac{2Q_{out_{1°step}} \bullet C_{out,Mg^{2+}_{1°step}}}{C_{NaOH_{2°step}}}$
$\text{Magma density}_{Mg(OH)_2 1°step} = \dfrac{M_{Mg(OH)_2 1°step}}{Q_{out_{1°step}}}$	$Q_{NaOH,added_{2°step}} = \dfrac{\left(C_{Ca(OH)_2 sol} - C_{NaOH_{pH=13}}\right) \bullet \left(Q_{out_{1°step}} + Q_{NaOH,stoic_{2°step}}\right)}{\left(C_{NaOH_{pH=13}} - C_{NaOH_{2°step}}\right)}$
$C_{out,Mg^{2+}_{1°step}} = \dfrac{Q_{feed_{1°step}} \bullet C_{feed,Mg^{2+}_{1°step}} \left(1 - \%_{Mg^{2+}_{1°step}}\right)}{Q_{NaOH_{1°step}} + Q_{feed_{1°step}}}$	$Q_{NaOH_{2°step}} = Q_{NaOH,stoic_{2°step}} + Q_{NaOH,Mg_{2°step}} + Q_{NaOH,added_{2°step}}$
$C_{out,Na^+_{1°step}} = \dfrac{Q_{feed_{1°step}} \bullet C_{feed,Na^+_{1°step}} + Q_{NaOH_{1°step}} \bullet C_{NaOH_{1°step}}}{Q_{out_{1°step}}}$	$Q_{out_{2°step}} = Q_{NaOH_{2°step}} + Q_{out_{1°step}}$
$C_{out,i^{th}_{1°step}} = \dfrac{Q_{feed_{1°step}} \bullet C_{feed,i^{th}_{1°step}}}{Q_{out_{1°step}}}$	
$C_{out,Ca^{2+}_{1°step}} = \dfrac{Q_{feed_{1°step}} \bullet C_{feed,Ca^{2+}_{1°step}} - Q_{feed_{1°step}} \bullet C_{feed,HCO_3^-_{1°step}}}{Q_{out_{1°step}}}$	$M_{Ca(OH)_2 2°step} = Q_{feed,Ca^{2+}_{2°step}} \bullet \%_{Ca^{2+}_{2°step}} \bullet MW_{Ca(OH)_2}$
$C_{out,HCO_3^-_{1°step}} = 0$	$\text{Magma density}_{Ca(OH)_2 2°step} = \dfrac{M_{Ca(OH)_2 2°step}}{Q_{out_{2°step}}}$
$M_{CaCO_3 1°step} = Q_{feed_{1°step}} \bullet C_{feed,HCO_3^-_{1°step}} \bullet MW_{CaCO_3}$	$C_{out,Na^+_{2°step}} = \dfrac{Q_{out_{1°step}} \bullet C_{out,Na^+_{1°step}} + Q_{NaOH_{2°step}} \bullet C_{NaOH_{2°step}}}{Q_{out_{2°step}}}$
	$C_{out,Mg^{2+}_{2°step}} = C_{out,HCO_3^-_{2°step}} = 0$
	$C_{out,i^{th}_{2°step}} = \dfrac{Q_{out_{1°step}} \bullet C_{out,i^{th}_{1°step}}}{Q_{out_{2°step}}}$
	$C_{out,Ca^{2+}_{2°step}} = \dfrac{Q_{out_{1°step}} \bullet C_{out,Ca^{2+}_{1°step}} \left(1 - \%_{Ca^{2+}_{2°step}}\right)}{Q_{out_{2°step}}}$
$Q_{HCl_{TOT}} = Q_{NaOH,added_{2°step}} \bullet C_{NaOH_{2°step}}$ $Q_{effluent} = Q_{out_{2°step}} + \dfrac{Q_{HCl_{TOT}}}{C_{HCl}}$	

A.3. Multi-Effect Distillation MED technical model

The technical model for the MED takes into account a Forward Feed configuration in which both feed water and vapour flow in the same direction. The MED unit comprises three different classes of effects for which different mass and energy equations are applied ((i) the first effect, (ii) the intermediate effects and (iii) the last effect with the end condenser). All equations are reported in Table C1. λ is the latent heat of water, h_{vap} is the enthalpy of the steam, h_{liq} is the enthalpy of the liquid water, h_{sw} is the enthalpy of the NaCl salt-water solution and $c_{p,sw}$ is the NaCl salt-water solution specific heat. The water properties are function of temperature, while the NaCl-water solution properties are functions of temperature and composition.

Table C1
Main mass and energy balance equations of the forward-feed MED model.

$M_{feed} = M_{dist} + M_{brine}$
$M_{feed} X_{feed} = M_{brine} X_{brine}$
$T_{vsat} = T - BPE(T, X_{brine})$
$T_{vsat}' = T_{vsat} - \Delta T_{demister}$
$T_c' = T_{vsat}' - \Delta T_{lines}$
$T_c = T_c' - \Delta T_{grav} - \Delta T_{acc}$
$M_s \lambda(T_s) + M_{feed} h_{sw}(T_{preh}[1], X_{feed}) = M_b[1] h_{sw}(T[1], X_b[1]) + (1 - \alpha_{cond}[1]) M_{vap}[1] h_{vap}(T_{vsat}'[1]) + \alpha_{cond}[1] M_{vap}[1]$
    $h_{liq}(T'_{vsat}[1])$
$M_b[i - 1] = M_d[i] + M_{fbrine}[i] + M_b[i]$
$M_{feed} X_{feed} = M_b[i] X_b[i]$
$M_{vap}[i] = M_d[i] + M_{fbrine}[i] + M_{fb}[i]$
$M_c[i - 1] + \alpha_{cond}[i] M_{vap}[i] + (1 - \alpha_{cond}[i - 1]) M_{vap}[i - 1] = M_{fb}[i] + M_c[i]$
$M_c[i - 1] h_{liq}(T_{v, sat}'[i - 1]) + \alpha_{cond}[i] M_{vap}[i] h_{liq}(T_{vsat}'[i]) + (1 - \alpha_{cond}[i - 1]) M_{vap}[i - 1] h_{liq}(T_c[i - 1]) = M_{fb}[i]$
    $h_{vap}(T'_{vsat}[i]) + M_c[i] h_{liq}(T'_{vsat}[i])$
$M_{fbrine}[i] \lambda(T_{brine, f}[i]) = M_{brine}[i - 1] c_{psw}(T_{mean}, X_b[i - 1])(T[i - 1] - T_{brine, f}[i])$
$M_{feed} c_{psw}(T_{mean}, X_f) (T_{preh}[i] - T_{preh}[i + 1]) = \alpha_{cond}[i] M_{vap}[i] \lambda(T'_{vsat}[i])$
$(1 - \alpha_{cond}[i - 1]) M_{vap}[i - 1] \lambda(T_c[i - 1]) + M_{fbrine}[i](h_{sw}(T[i - 1], X_b[i - 1]) - h_{vap}(T_{vsat}'[i])) + M_b[i](h_{sw}(T[i - 1], X_b[i - 1]) - h_{sw}(T[i], X_b[i])) = M_d[i](h_{vap}(T_{vsat}'[i]) - h_{sw}(T[i - 1], X_b[i - 1]))$
$(1 - \alpha_{cond}[N - 1]) M_{vap}[N - 1] \lambda(T_c[N - 1]) + M_{fb}[N] h_{vap}(T_{vsat}'[N]) + M_b[N - 1] h_{sw}(T[N - 1], X_b[N - 1]) = M_b[N]$
    $h_{sw}(T[N], X_b[N]) + M_{vap}[N] h_{vap}(T'_{vsat}[N])$
$M_{cw} c_{Psw}(\overline{T_{cw}}, X_{feed}) (T_{cw,out} - T_{cw,in}) = M_{vap}[N] \lambda(T_c'[N])$

Firstly, global mass and salinity balances are employed to calculate the brine flow rate (M_{brine}), the distillate flow rate (M_{dist}) and the brine salinity (X_{brine}), assuming that the distillate is pure water. From this point onwards, the mass flow rate, temperature and pressure are computed for each effect. As for the temperature profiles, six main quantities must be taken into account and computed: (i) temperature of the brine generated in the effect (T), (ii) temperature reached by the feed in the preheater of the effect (T_{preh}), (iii) temperature of the saturated vapour generated in the effect (T_{vsat}), (iv) temperature of the vapour after crossing the demister (T'_{vsat}), (v) temperature of the vapour after crossing the connecting lines (T'_c) and (vi) condensation temperature of the vapour in the following effect (T_c). All six quantities are connected by means of the the boiling point elevation (BPE) and the pressure drops, leading to temperature drops ($\Delta T_{demister}$, ΔT_{lines}, ΔT_{grav}, ΔT_{acc}), in the case of saturated vapour. The Pitzer model is employed to estimate the BPE.

Among the three classes of effects, the first one is the only one which receives heat from an external source (M_s at temperature equal to T_s) and where the feed stream (M_{feed} at a concentration equal to X_{feed}) has been through all the preheaters. The feed of the first effect is sprayed onto a tube bundle whereas M_s circulates within the tubes. The vapour (M_{vap}) is generated by the partial evaporation of the feed stream (M_d). The vapour then crosses the demister and the first preheater, where it partially condenses. The part that does not condense is fed to next effect where it acts as the heating source. The remaining brine that exits the first effect (M_b at a concentration equal to X_b) is also fed to the next effect where it is sprayed on the external surface of the tube bundle. As already mentioned, the modelling of the intermediate effects is slightly different. It comprises two energy balances on the preheater and on the heat exchanger required to calculate the condensed fraction on the preheater tube surface (α_{cond}) and M_d, respectively. Furthermore, other two vapour contributions have to be taken into account: the vapour produced by the inlet brine flash. As for the modelling of the last effect, the latter does not have any preheater and all the vapour is sent directly to the end condenser, where it condenses completely. This can be mathematically translated into different energy balances on the effect and on the last flashing box, since the total M_{vap} in the last effect condenses in the end condenser and then collected in the flash box. The brine M_b that exits the last effect is the generated in the last effect is the final brine of the entire MED plant. The condensate of the flash box M_c, on the other hand, is the final distillate of the plant. These outlets however have to respect the global mass balance equations. As far as the end condenser is concerned its feed is used to condensate the vapour. The required total cooling water flow rate (M_{cw}) is computed by means of the heat balance and the surplus ($M_{cw} - M_{feed}$) is cooled down and reused.

Table C2 reports the equations to calculate the areas of the heat exchangers, the areas of the preheaters and the areas of the end condenser where $DTML_{preh}$ and $DTML_{cond}$ are the temperature logarithmic mean in the preheater and in the condenser and U_{cond} and U_{evap} are the heat transfer co-efficients for the condenser and the evaporator, respectively.

Table C2
Equations to calculate the heat exchangers, preheaters and end condenser areas of the MED plant.

$$A_{hx}[0] = \frac{M_{feed}c_{P_{sw}}(T_{mean}, X_f)(T[1] - T_{preh}[1]) + M_d[1]\lambda(T_{vsat}[1])}{U_{evap}(T[1])(T_{steam} - T[1])}$$

$$A_{hx}[i] = \frac{(1 - \alpha_{cond}[i-1])M_{vap}[i-1]\lambda(T_c[i-1])}{U_{evap}(T[i])(T_c[i-1] - T[i])}$$

$$A_{preh}[i] = \frac{\alpha_{cond}[i]\,M_{vap}[i]\,\lambda(T'_{vsat}[i])}{U_{cond}(T'_{vsat}[i])\,DTML_{preh}}$$

$$A_{cond} = \frac{M_{cw}\,c_{P_{sw}}(T_{cw}, X_{feed})\,(T_{cw,out} - T_{cw,in})}{U_{cond}(T'_c[N])\,DTML_{cond}}$$

A.4. NaCl Thermal Crystallizer NTC technical model

The technical model of the NaCl Thermal Crystallizer is based on simple mass and energy balance equations where M is the generic mass flow rate and Q is the generic volumetric flow rate. However, the model was developed in such a way that it depends on the previous MED plant and takes into account the desired recovery of NaCl salt %$_{recovery}$ achieved globally from the coupling MED-NTC. It is therefore possible to calculate the mass flow rate of salt $M_{out, salt_{NTC}}$ and of brine $M_{out, brine_{NTC}}$ both exiting the crystallizer. Subsequently, logical conditions are taken into account depending on the NF membrane rejection correction factor α. By means of PHREEQC software it is possible to observe how different compounds precipitate when different NF ion rejections are considered. Therefore, according to the value of α, a specific set of equations is used related to the specific compound that precipitates. Finally, the molar concentration of the generic ion i in the brine $C_{out, i^{th}, brine_{NTC}}$ is calculated along with the mass distillate flow rate $M_{out, dist_{NTC}}$. As for the energy balance equations, the sensible heat $H_{sens_{NTC}}$ and latent heat $H_{evap_{NTC}}$ are computed where T_{NTC} is the operating temperature of the crystallizer and T_{IN} is the temperature of the inlet stream of the crystallizer.

Table D1
Mass and Energy balance equations of the NaCl Thermal Crystallizer plant.

$Q_{feed,Na^+{}_{MED}} = M_{feed,MED} \bullet C_{feed,Na^+{}_{MED}}$

$Q_{out,Na^+,salt_{NTC}} = \%_{recovery} \bullet Q_{feed,Na^+{}_{MED}}$

$M_{out, salt_{NTC}} = Q_{out, Na^+, salt_{NTC}} \bullet MW_{NaCl}$

$Q_{out,Na^+,brine_{NTC}} = \dfrac{M_{feed,NTC} \bullet C_{feed,Na^+{}_{NTC}} - Q_{out,Na^+,salt_{NTC}} \bullet MW_{Na^+}}{MW_{Na^+}}$

$M_{out,brine_{NTC}} = \dfrac{M_{feed,NTC} \bullet MW_{NaCl} - Q_{out,Na^+,salt_{NTC}}}{C_{NaCl_{sat}}}$

$\alpha = 0.1$ or 0.7

$C_{out,SO_4{}^{2-},brine_{NTC}} = \dfrac{M_{feed,NTC} \bullet C_{feed,SO_4{}^{2-}{}_{NTC}}}{M_{out,brine_{NTC}} \bullet MW_{SO_4{}^{2-}}}$

$C_{out,Na_2SO_4,prec_{NTC}} = C_{out,SO_4{}^{2-},brine_{NTC}} - C_{Na_2SO_{4sat}}$

$C_{out, Na^+, brine_{NTC}} = C_{NaCl_{sat}}$ if Na_2SO_4 precipitates

$C_{out, Na^+, brine_{NTC}} = 2C_{out, Na_2SO_4, prec_{NTC}}$ if Na_2SO_4 does not precipitate

$\alpha \neq 0.1$ or 0.7

if $C_{feed,Ca^{2+}{}_{NTC}} > C_{feed,SO_4{}^{2-}{}_{NTC}}$

$C_{out, Ca^{2+}, brine_{NTC}} = C_{Na_2Ca(SO_4)_{2sat}}$

$C_{out,Na_2Ca(SO_4)_2,prec_{NTC}} = \dfrac{M_{feed,NTC} \bullet C_{feed,Ca^{2+}{}_{NTC}}}{M_{out,brine_{NTC}} \bullet MW_{Ca^{2+}}} - C_{Na_2Ca(SO_4)_{2sat}}$

if $C_{feed,Ca^{2+}{}_{NTC}} < C_{feed,SO_4{}^{2-}{}_{NTC}}$

$C_{out, Ca^{2+}, brine_{NTC}} = 0$

(continued on next page)

Table D1 (*continued*)

$$Q_{out,Na_2SO_4,prec_{NTC}} = M_{feed,NTC} \bullet C_{feed,SO_4^{2-}_{NTC}} - M_{out,brine_{NTC}} \bullet C_{Na_2SO_{4sat}}$$

$$C_{out,Na_2Ca(SO_4)_2,prec_{NTC}} = \frac{M_{feed,NTC} \bullet C_{feed,Ca^{2+}_{NTC}}}{M_{out,brine_{NTC}}}$$

$$C_{out,Na^+,brine_{NTC}} = C_{NaCl_{sat}} - 2C_{out,Na_2Ca(SO_4)_2,prec_{NTC}}$$

$$C_{out,SO_4^{2-},brine_{NTC}} = \frac{M_{feed,NTC} \bullet C_{feed,SO_4^{2-}_{NTC}} - 2C_{out,Na_2Ca(SO_4)_2,prec_{NTC}} \bullet M_{out,brine_{NTC}}}{M_{out,brine_{NTC}}}$$

$$C_{out,i^{th},brine_{NTC}} = \frac{M_{feed,NTC} \bullet C_{feed,i^{th}_{NTC}}}{M_{out,brine_{NTC}}}$$

$$C_{out,Cl^-,brine_{NTC}} = \frac{M_{feed,NTC} \bullet C_{feed,Cl^-_{NTC}} - Q_{out,Na^+,salt_{NTC}}}{M_{out,brine_{NTC}}}$$

$$M_{out,dist_{NTC}} = M_{feed,NTC} - Q_{out,Na^+,salt_{NTC}} \bullet MW_{NaCl} - M_{out,brine_{NTC}}$$

$$H_{sens_{NTC}} = M_{feed,NTC} \bullet Cp_{NaCl\,sol_{sat}} \bullet (T_{NTC} - T_{IN})$$

$$H_{evap_{NTC}} = M_{out,dist_{NTC}} \bullet Cp_{NaCl\,sol_{sat}} \bullet (T_{NTC} - T_{IN})\lambda_{dist}$$

$$H_{TOT_{NTC}} = H_{sens_{NTC}} + H_{evap_{NTC}}$$

Appendix B. Economic models

B.1. Nanofiltration NF economic model

The equations for the calculation of the capital and operating costs are reported in Table E1.

Table E1
Equations for the calculation of capEX and opEX of the NF unit.

capEX equations for NF*	opEX equations for NF
$C_{civil,NF} = \frac{(1034.4V_{feed,NF} + 1487x_{vessel})CEPCI_{ref}}{CEPCI_{current}} \frac{(1+i)^{n_{civil}} i}{(1+i)^{n_{civil}} - 1}$ *****	$C_{elec,NF} = \frac{Cost_{elec} \bullet V_{feed,NF} \bullet N_{oper,hours}}{\%_{eff}}(cons_{memb,syst} + P_{feed,NF})$
$C_{mech,NF} = \frac{\left(4329.6V_{feed,NF}^{0.85} + 1089.6x_{vessel}\right)CEPCI_{ref}}{CEPCI_{current}} \frac{(1+i)^{n_{mech}} i}{(1+i)^{n_{mech}} - 1}$	$C_{chem,NF} = Cost_{chem,NF} \bullet V_{permeate} \bullet N_{oper,hours}$
$C_{electro,NF} = \frac{(1.68 \bullet 10^6 + 64.8P_{feed,NF} \bullet V_{feed,NF})CEPCI_{ref}}{CEPCI_{current}} \frac{(1+i)^{n_{electro}} i}{(1+i)^{n_{electro}} - 1}$	$C_{main,NF} = 2\ \%\ capEX_{NF}$
$C_{memb,NF} = \frac{1200x_{vessel} \bullet CEPCI_{ref}}{CEPCI_{current}} \frac{(1+i)^{n_{memb}} i}{(1+i)^{n_{memb}} - 1}$	$C_{quality,NF} = 2\ \%\ capEX_{NF}$
	$C_{install,NF} = 2\ \%\ capEX_{NF}$
$capEX_{NF} = C_{civil,NF} + C_{mech,NF} + C_{electro,NF} + C_{memb,NF}$	$opEX_{NF} = C_{elec,NF} + C_{chem,NF} + C_{main,NF} + C_{quality,NF} + C_{install,NF}$

* The Verbene Cost Model equations were employed.
** CEPCI$_{ref}$ is referred to 2001 (394.3).
*** CEPCI$_{current}$ is referred to 2021 (754.0).

Among the capital costs, $C_{civil,NF}$ [€/y] represents the cost for buildings housing the plant, $C_{mech,NF}$ [€/y] is the cost for pumps, filters and piping, $C_{electro,NF}$ [€/y] is the costs for the energy supply systems, $C_{memb,NF}$ [€/y] is the investment for the membrane modules, $V_{feed,NF}$ [m³/h] is the feed flow rate, n_{vessel} is the number of NF vessels, $P_{feed,NF}$ [Pa] is the feed pressure and CEPCI is the chemical engineering price index. All capEX contributions are depreciated considering a specific depreciation period (n_{civil} for $C_{civil,NF}$, $n_{mech} = n_{electro}$ for $C_{mech,NF}$ and $C_{electro,NF}$, n_{memb} for the membrane) with a discount rate i. Among the operating costs, $C_{elec,NF}$ [€/y] is the cost of electrical energy consumption, $C_{chem,NF}$ [€/y] is the chemical consumption, $C_{main,NF}$ [€/y] is the cost of maintenance, $C_{quality,NF}$ [€/y] is the cost for quality control and $C_{install,NF}$ [€/y] is the cost of daily operation. Cost$_{elec}$ [€/kWh] is the specific cost of electricity, $\%_{eff}$ is the pump efficiency (80 %), $N_{oper,hours}$ [h/y] is the annual number of operating hours, $cons_{memb,syst}$ is the specific energy consumption for a membrane system (40 Wh/m³ of feed). Cost$_{chem,NF}$ (0.023 €/m³ of permeate) is the specific cost of chemicals employed and $V_{permeate}$ [m³/h] is the NF permeate flow rate.

B.2. Magnesium Reactive Crystallizer MRC economic model

Equations to compute the capital costs of the MRC unit are reported in Table F1 where C_p^0 [€] is the purchase cost in standard conditions for the crystallizer and the filter, Vol_{cryst} [m³] is the volume of crystallizer, A_{filter} [m²] is the area of the filter, F_{BM} is the global correction factor (1.6 and 1.65 for the crystallizer and the filter, respectively), C_{BM} [€] is the bare module cost, $\alpha_{cont} = 15\ \%$ and $\alpha_{fee} = 5\ \%$ are the two correction factors to account contingency and fee, respectively. C_{TM} [€] is the total module cost which is depreciated within a period (n_{MRC}) with a discount rate i. Among the operating costs of the MRC, $C_{elec,MRC}$ [€/y] is the cost of energy consumption for pumping and the drum filter, Power$_{MRC,TOT}$ [kW] is the total consumed power, $C_{NaOH,MRC}$ [€/y] is the cost of reaction chemicals, Cost$_{NaOH}$ [€/ton] is the specific cost of NaOH, $Q_{NaOH,TOT}$ [ton/h] is the mass flow rate of NaOH, (iii) $C_{HCl,MRC}$ [€/y] is the cost of chemicals for the neutralization step, Cost$_{HCl}$ [€/ton] is the specific cost of HCl and $Q_{HCl,TOT}$ [ton/h] is the mass flow rate of HCl.

Table F1
Equations for the calculation of capEX and opEX of the MRC unit.

capEX equations for MRC*	opEX equations for MRC
$C_{p,Cryst}^0 = 10^{(4.509+0.173Log_{10}(Vol_{cryst})+0.134*(Log_{10}(Vol_{cryst}))^2)}$	$C_{elec,MRC} = \frac{Cost_{elec} \bullet Power_{TOT,MRC} \bullet N_{oper,hours}}{\%_{eff}}$
$C_{p,filter}^0 = 10^{(4.812+0.286Log_{10}(A_{filter})+0.042*(Log_{10}(A_{filter}))^2)}$	$C_{NaOH,MRC} = Cost_{NaOH} \bullet Q_{NaOH,TOT} \bullet N_{oper,hours}$
	$C_{HCl,MRC} = Cost_{HCl} \bullet Q_{HCl,TOT} \bullet N_{oper,hours}$

Table F1 (*continued*)

capEX equations for MRC[*]	opEX equations for MRC
$C_{BM,Cryst} = \dfrac{C^0_{p,Cryst} \bullet CEPCI_{ref}}{CEPCI_{current}} \left(F_{BM,cryst}\right)$ [**,***] $C_{BM,filter} = \dfrac{C^0_{p,filter} \bullet CEPCI_{ref}}{CEPCI_{current}} \left(F_{BM,filter}\right)$ $C_{TM, MRC} = (C_{BM, Cryst} + C_{BM, filter})(1 + \alpha_{cont} + \alpha_{fee})$ $capEX_{MRC} = C_{TM,MRC}\dfrac{(1+i)^{n_{MRC}}i}{(1+i)^{n_{MRC}} - 1}$	$opEX_{MRC} = C_{elec, MRC} + C_{NaOH, MRC} + C_{HCl, MRC}$

[*] The Bare Module Cost Technique equations were employed.
[**] CEPCI$_{ref}$ is referred to 2001 (394.3).
[***] CEPCI$_{current}$ is referred to 2021 (754.0).

B.3. Multi-Effect Distillation MED economic model

Equations to compute the capital costs of the MED unit are reported in Table G1 where N_{evap} is the number of evaporators, N_{preh} is the number of preheaters, $N_{flashbox}$ is the number of flashboxes and N_{cond} is the number of condensers. F_{BM} is the global correction factor, $\alpha_{cont} = 15\%$ and $\alpha_{fee} = 5\%$ are the two correction factors to account contingency and fee, C_{BM} [€] is the bare module cost, C_{TM} [€] is the total module cost depreciated within a period (n_{MED}) with a discount rate i. As for the operating costs, $C_{elec, MED}$ [€/y] is the electric energy consumption, $Cons_{elec, MED}$ [kWh/m³ of distillate] is the specific energy consumption of the MED unit, $V_{dist, MED}$ [m³/h] is the volumetric flow rate of the produced distillate, $C_{thermal, MED}$ [€/y] is the thermal energy consumption, $Cost_{heat}$ [€/kWh] is the specific cost of heat of the MED, $Cons_{heat, MED}$ [kW] is the required thermal energy, $C_{chem, MED}$ is the chemical consumption required for cleaning, anti-scaling and anti-foaming, Q_i is the quantity consumed of the ith chemical [ton/h] and $Cost_i$ is the specific cost of the ith chemical [€/ton].

Table G1
Equations for the calculation of capEX and opEX of the MED unit.

capEX equations for MED[*]	opEX equations for MED
$C^0_{p, evap} = 10^{(4.325-0.303Log_{10}(A_{evap})+0.163(Log_{10}(A_{evap}))^2)}$ $C^0_{p, preh} = 10^{(4.325-0.303Log_{10}(A_{preh})+0.163(Log_{10}(A_{preh}))^2)}$ $C^0_{p, flash} = 10^{(3.557+0.378Log_{10}(A_{flash})+0.091(Log_{10}(A_{flash}))^2)}$ $C^0_{p, cond} = 10^{(4.325-0.303Log_{10}(A_{cond})+0.163(Log_{10}(A_{cond}))^2)}$ $C_{BM,evap} = N_{evap}\dfrac{C^0_{p,evap} \bullet CEPCI_{ref}}{CEPCI_{current}}\left(F_{BM,evap}\right)$ [**,***] $C_{BM,preh} = N_{preh}\dfrac{C^0_{p,preh} \bullet CEPCI_{ref}}{CEPCI_{current}}\left(F_{BM,preh}\right)$ $C_{BM,flash} = N_{flash}\dfrac{C^0_{p,flash} \bullet CEPCI_{ref}}{CEPCI_{current}}\left(F_{BM,flash}\right)$ $C_{BM,cond} = N_{cond}\dfrac{C^0_{p,cond} \bullet CEPCI_{ref}}{CEPCI_{current}}\left(F_{BM,cond}\right)$ $C_{TM, MRC} = (C_{BM, evap} + C_{BM, preh} + C_{BM, flash} + C_{BM, cond})(1 + \alpha_{cont} + \alpha_{fee})$ $capEX_{MED} = C_{TM,MED}\dfrac{(1+i)^{n_{MED}}i}{(1+i)^{n_{MED}} - 1}$	$C_{elec, MED} = Cost_{elec} \bullet Cons_{elect, MED} \bullet V_{dist, MED} \bullet N_{oper, hours}$ $C_{thermal, MED} = Cost_{heat} \bullet Cons_{heat, MED} \bullet N_{oper, hours}$ $C_{chem, MED} = (Cost_{pre-Chlorine} \bullet Q_{pre-Chlorine} + Cost_{antiscalant} \bullet Q_{antiscalant} + Cost_{antifoaming} \bullet Q_{antifoaming} + Cost_{Ca(OH)2} \bullet Q_{Ca(OH)2} + Cost_{polyelectrolyte} \bullet Q_{polyelectrolyte} + Cost_{CO2} \bullet Q_{CO2} + Cost_{post-Chlorine} \bullet Q_{post-Chlorine})N_{oper, hours}$ $opEX_{MED} = C_{elec, MED} + C_{thermal, MED} + C_{chem, MED}$

[*] The Bare Module Cost Technique equations were employed.
[**] CEPCI$_{ref}$ is referred to 2001 (394.3).
[***] CEPCI$_{current}$ is referred to 2021 (754.0).

B.4. NaCl Thermal Crystallizer NTC economic model

Equations to compute the capital costs of the NTC unit are reported in Table H1 where Vol_{cryst} [m³] is the volume of NTC, $F_{BM, NTC}$ is the global correction factor equal to 1.6 and contingency and fee ($\alpha_{cont} = 15\%$ and $\alpha_{fee} = 5\%$) and $C_{TM, NTC}$ [€] is the total module cost depreciated within a period (n_{NTC}) with a discount rate i. Among the operating costs of the NTC unit, $C_{elec, NTC}$ [€/y] is the cost of electric energy consumption for pumping, $Cons_{elec, NTC}$ [kWh/m³ of distillate] is the specific energy consumption of the crystallizer, $V_{dist, NTC}$ [m³/h] is the volumetric flow rate of the produced distillate, $C_{thermal, NTC}$ [€/y] is the cost of thermal energy required for the precipitation of NaCl crystals, $Cost_{heat}$ [€/kWh] is the specific cost of heat of the NTC, $Cons_{heat, NTC}$ [kW] is the required thermal energy, $C_{brine disposal}$ [€/y] is the disposal cost of the final brine, $Cost_{brine disp}$ [€/m³ of brine] is the specific cost of brine disposal and $V_{brine, NTC}$ [m³/h] is the volumetric flow rate of the final brine.

Table H1
Equations for the calculation of capEX and opEX of the NTC unit.

capEX equations for NTC[*]	opEX equations for NTC
$C^0_{p, NTC} = 10^{(4.509+0.173*Log_{10}(Vol_{NTC})+0.134*(Log_{10}(Vol_{NTC}))^2)}$ $C_{BM,NTC} = \dfrac{C^0_{p,NTC} \bullet CEPCI_{ref}}{CEPCI_{current}}\left(F_{BM,NTC}\right)$ [**,***] $C_{TM, NTC} = (C_{BM, NTC})(1 + \alpha_{cont} + \alpha_{fee})$ $capEX_{NTC} = C_{TM,NTC}\dfrac{(1+i)^{n_{NTC}}i}{(1+i)^{n_{NTC}} - 1}$	$C_{elec, NTC} = Cost_{elec} \bullet Cons_{elect, NTC} \bullet V_{dist, NTC} \bullet N_{oper, hours}$ $C_{thermal, NTC} = Cost_{heat} \bullet Cons_{heat, NTC} \bullet N_{oper, hours}$ $C_{brine disposal} = Cost_{brine disp} \bullet V_{brine, NTC} \bullet N_{oper, hours}$ $opEX_{NTC} = C_{elec, NTC} + C_{thermal, NTC} + C_{brine disposal}$

[*] The Bare Module Cost Technique equations were employed.
[**] CEPCI$_{ref}$ is referred to 2001 (394.3).

*** CEPCI$_{current}$ is referred to 2021 (754.0).

References

[1] A. Panagopoulos, A comparative study on minimum and actual energy consumption for the treatment of desalination brine, Energy 212 (2020), 118733, https://doi.org/10.1016/j.energy.2020.118733.

[2] E. Jones, M. Qadir, M.T.H. van Vliet, V. Smakhtin, S. mu Kang, The state of desalination and brine production: a global outlook, Sci. Total Environ. 657 (2019) 1343–1356, https://doi.org/10.1016/j.scitotenv.2018.12.076.

[3] D. Xevgenos, K. Moustakas, D. Malamis, M. Loizidou, An overview on desalination & sustainability: renewable energy-driven desalination and brine management, Desalin. Water Treat. 57 (2016) 2304–2314, https://doi.org/10.1080/19443994.2014.984927.

[4] S. van Wyk, A.G.J. van der Ham, S.R.A. Kersten, Potential of supercritical water desalination (SCWD) as zero liquid discharge (ZLD) technology, Desalination 495 (2020), 114593, https://doi.org/10.1016/j.desal.2020.114593.

[5] M. Bornhoft, P. Takach, Consideration for implementaing a zero liquid discharge program, Water Technol. (2018) 1–18. https://www.watertechonline.com/wastewater/article/15550690/considerations-for-implementing-a-zero-liquid-discharge-program.

[6] A. Panagopoulos, K.J. Haralambous, M. Loizidou, Desalination brine disposal methods and treatment technologies - a review, Sci. Total Environ. 693 (2019), 133545, https://doi.org/10.1016/j.scitotenv.2019.07.351.

[7] M.O. Mavukkandy, C.M. Chabib, I. Mustafa, A. Al Ghaferi, F. AlMarzooqi, Brine management in desalination industry: from waste to resources generation, Desalination 472 (2019), 114187, https://doi.org/10.1016/j.desal.2019.114187.

[8] J.M. Arnal, M. Sancho, I. Iborra, J.M. Gozálvez, A. Santafé, J. Lora, Concentration of brines from RO desalination plants by natural evaporation, Desalination 182 (2005) 435–439, https://doi.org/10.1016/j.desal.2005.02.036.

[9] K.L. Petersen, A. Paytan, E. Rahav, O. Levy, J. Silverman, O. Barzel, D. Potts, E. Bar-Zeev, Impact of brine and antiscalants on reef-building corals in the Gulf of Aqaba – potential effects from desalination plants, Water Res. 144 (2018) 183–191, https://doi.org/10.1016/j.watres.2018.07.009.

[10] U.S. Department of the Interior Bureau of Reclamation, Brine-Concentrate Treatment and Disposal Options Report - Part 1. http://s3-us-west-2.amazonaws.com/ucldc-nuxeo-ref-media/69c012ec-cae3-4b58-a56a-3a712960a918, 2009.

[11] J.H. Tsai, F. Macedonio, E. Drioli, L. Giorno, C.Y. Chou, F.C. Hu, C.L. Li, C. J. Chuang, K.L. Tung, Membrane-based zero liquid discharge: myth or reality? J. Taiwan Inst. Chem. Eng. 80 (2017) 192–202, https://doi.org/10.1016/j.jtice.2017.06.050.

[12] I. Ersever, V. Ravindran, M. Pirbazari, Biological denitrification of reverse osmosis brine concentrates: I. Batch reactor and chemostat studies, J. Environ. Eng. Sci. 6 (2007) 503–518, https://doi.org/10.1139/S07-021.

[13] A. Subramani, J.G. Jacangelo, Treatment technologies for reverse osmosis concentrate volume minimization: a review, Sep. Purif. Technol. 122 (2014) 472–489, https://doi.org/10.1016/j.seppur.2013.12.004.

[14] M. Ahmed, W.H. Shayya, D. Hoey, J. Al-Handaly, Brine disposal from reverse osmosis desalination plants in Oman and the United Arab Emirates, Desalination 133 (2001) 135–147, https://doi.org/10.1016/S0011-9164(01)80004-7.

[15] R. Kaplan, D. Mamrosh, H.H. Salih, S.A. Dastgheib, Assessment of desalination technologies for treatment of a highly saline brine from a potential CO2 storage site, Desalination 404 (2017) 87–101, https://doi.org/10.1016/j.desal.2016.11.018.

[16] Z. Wang, A. Deshmukh, Y. Du, M. Elimelech, Minimal and zero liquid discharge with reverse osmosis using low-salt-rejection membranes, Water Res. 170 (2020), 115317, https://doi.org/10.1016/j.watres.2019.115317.

[17] A. Panagopoulos, Beneficiation of saline effluents from seawater desalination plants: fostering the zero liquid discharge (ZLD) approach - a techno-economic evaluation, J. Environ. Chem. Eng. 9 (2021), https://doi.org/10.1016/j.jece.2021.105338.

[18] A. Panagopoulos, Techno-economic assessment of zero liquid discharge (ZLD) systems for sustainable treatment, minimization and valorization of seawater brine, (n.d.). doi:10.1016/j.jenvman.2022.114488.

[19] X. Ji, E. Curcio, S. Al Obaidani, G. Di Profio, E. Fontananova, E. Drioli, Membrane distillation-crystallization of seawater reverse osmosis brines, Sep. Purif. Technol. 71 (2010) 76–82, https://doi.org/10.1016/j.seppur.2009.11.004.

[20] Q. Chen, M. Burhan, M.W. Shahzad, D. Ybyraiymkul, F.H. Akhtar, Y. Li, K.C. Ng, A zero liquid discharge system integrating multi-effect distillation and evaporative crystallization for desalination brine treatment, Desalination 502 (2021), 114928, https://doi.org/10.1016/j.desal.2020.114928.

[21] G. Al Bazedi, R.S. Ettouney, S.R. Tewfik, M.H. Sorour, M.A. El-Rifai, Salt recovery from brine generated by large-scale seawater desalination plants, Desalin. Water Treat. 52 (2014) 4689–4697, https://doi.org/10.1080/19443994.2013.810381.

[22] M. Turek, K. Mitko, M. Chorzewska, P. Dydo, Use of the desalination brines in the saturation of membrane electrolysis feed, Desalin. Water Treat. 51 (2013) 2749–2754, https://doi.org/10.1080/19443994.2012.749372.

[23] M. Turek, P. Dydo, R. Klimek, Salt production from coal-mine brine in ED-evaporation-crystallization system, Desalination 184 (2005) 439–446, https://doi.org/10.1016/j.desal.2005.03.047.

[24] W. Zhang, M. Miao, J. Pan, A. Sotto, J. Shen, C. Gao, B. Van Der Bruggen, Process economic evaluation of resource valorization of seawater concentrate by

[25] M. Kieselbach, T. Hogen, S.U. Geißen, T. Track, D. Becker, H.J. Rapp, J. Koschikowski, J. Went, H. Horn, F. Saravia, A. Bauer, R. Schwantes, D. Pfeifle, N. Heyn, M. Weissroth, B. Fitzke, Brines from industrial water recycling: new ways to resource recovery, J. Water Reuse Desalin. 10 (2020) 443–461, https://doi.org/10.2166/wrd.2020.033.

[26] D. von Eiff, P.W. Wong, Y. Gao, S. Jeong, A.K. An, Technical and economic analysis of an advanced multi-stage flash crystallizer for the treatment of concentrated brine, Desalination 503 (2021), 114925, https://doi.org/10.1016/j.desal.2020.114925.

[27] D. Xevgenos, P. Michailidis, K. Dimopoulos, M. Krokida, M. Loizidou, Design of an innovative vacuum evaporator system for brine concentration assisted by software tool simulation, Desalin. Water Treat. 53 (2015) 3407–3417, https://doi.org/10.1080/19443994.2014.948660.

[28] D. Xevgenos, A. Vidalis, K. Moustakas, D. Malamis, M. Loizidou, Sustainable management of brine effluent from desalination plants: the SOL-BRINE system, Desalin. Water Treat. 53 (2015) 3151–3160, https://doi.org/10.1080/19443994.2014.933621.

[29] M. Turek, P. Dydo, R. Klimek, Salt production from coal-mine brine in NF - evaporation - crystallization system, Desalination 221 (2008) 238–243, https://doi.org/10.1016/j.desal.2007.01.080.

[30] RCE, in: Deutsches Zentrum für Luft- und Raumfahrt, 2021, pp. 1–6. https://rcenvironment.de/.

[31] F. Macedonio, C.A. Quist-Jensen, O. Al-Harbi, H. Alromaih, S.A. Al-Jlil, F. Al Shabouna, E. Drioli, Thermodynamic modeling of brine and its use in membrane crystallizer, Desalination 323 (2013) 83–92, https://doi.org/10.1016/j.desal.2013.02.009.

[32] INTERVENTO DI RICERCA E RIDUZIONE DELLE PERDITE NEL SISTEMA DI ADDUZIONE E DISTRIBUZIONE IDRICA NELL'ISOLA DI PANTELLERIA, (n.d.). http://www.comunepantelleria.it/gare/68550928DE/R.1 Relazione illustrativa Consistenza della rete idrica.pdf.

[33] Y. Roy, D.M. Warsinger, J.H. Lienhard, Effect of temperature on ion transport in nanofiltration membranes: diffusion, convection and electromigration, Desalination 420 (2017) 241–257, https://doi.org/10.1016/j.desal.2017.07.020.

[34] N. Hilal, H. Al-Zoubi, N.A. Darwish, A.W. Mohammad, M.Abu Arabi, A comprehensive review of nanofiltration membranes: Treatment, pretreatment, modelling, and atomic force microscopy, Desalination 170 (2004) 281–308, https://doi.org/10.1016/j.desal.2004.01.007.

[35] S. Jamaly, N.N. Darwish, I. Ahmed, S.W. Hasan, A short review on reverse osmosis pretreatment technologies, Desalination 354 (2014) 30–38, https://doi.org/10.1016/j.desal.2014.09.017.

[36] A.E. Abdullatef, M. Farooque, G. Al-Otaibi, M. Kither, S.Al Khamis, Optimum nanofiltration membrane arrangements in seawater pretreatment - part-I, Desalin. Water Treat. 28 (2011) 270–286, https://doi.org/10.5004/dwt.2011.1243.

[37] U.S. DEPARTMENT OF THE INTERIOR Bureau of Reclamation, Two-Pass Nanofiltration Seawater Desalination Prototype Testing and Evaluation. https://www.usbr.gov/research/dwpr/reportpdfs/report158.pdf, 2013.

[38] J. Luo, Y. Wan, Effects of pH and salt on nanofiltration-a critical review, J. Membr. Sci. 438 (2013) 18–28, https://doi.org/10.1016/j.memsci.2013.03.029.

[39] B.A. Abdelkader, M.A. Antar, Z. Khan, Nanofiltration as a pretreatment step in seawater desalination: a review, Arab. J. Sci. Eng. 43 (2018) 4413–4432, https://doi.org/10.1007/s13369-018-3096-3.

[40] D. Zhou, L. Zhu, Y. Fu, M. Zhu, L. Xue, Development of lower cost seawater desalination processes using nanofiltration technologies - a review, Desalination 376 (2015) 109–116, https://doi.org/10.1016/j.desal.2015.08.020.

[41] A.M. Hassan, M.A.K. Al-Sofi, A.S. Al-Amoudi, A.T.M. Jamaluddin, A.M. Farooque, A. Rowaili, A.G.I. Dalvi, N.M. Kither, G.M. Mustafa, I.A.R. Al-Tisan, New approach to membrane and thermal seawater desalination processes using nanofiltration membranes (part 1), Water Supply 17 (1999) 145–161.

[42] G.U. Semblante, J.Z. Lee, L.Y. Lee, S.L. Ong, H.Y. Ng, Brine pre-treatment technologies for zero liquid discharge systems, Desalination 441 (2018) 96–111, https://doi.org/10.1016/j.desal.2018.04.006.

[43] M. Turek, W. Gnot, Precipitation of magnesium hydroxide from brine, Ind. Eng. Chem. Res. 34 (1995) 244–250, https://doi.org/10.1021/ie00040a025.

[44] M.H. Gong, M. Johns, E. Fridjonsson, P. Heckley, in: Magnesium Recovery from Desalination Brine, 2018, pp. 49–54. http://ceed.wa.edu.au/wp-content/uploads/2018/09/9.Gong_.WaterCorp.MagnesiumRecovery.pdf.

[45] F. Vassallo, D. La Corte, A. Cipollina, A. Tamburini, G. Micale, High purity recovery of magnesium and calcium hydroxides from waste brines, Chem. Eng. Trans. 86 (2021) 931–936, https://doi.org/10.3303/CET2186156.

[46] F. Vassallo, D. La Corte, N. Cancilla, A. Tamburini, M. Bevacqua, A. Cipollina, G. Micale, A pilot-plant for the selective recovery of magnesium and calcium from waste brines, Desalination 517 (2021), 115231, https://doi.org/10.1016/j.desal.2021.115231.

[47] B. Rahimi, H.T. Chua, Introduction to desalination, low grade heat driven multi-effect distill, Desalination (2017) 1–17, https://doi.org/10.1016/b978-0-12-805124-5.00001-2.

[48] A. Ophir, F. Lokiec, Advanced MED process for most economical sea water desalination, Desalination 182 (2005) 187–198, https://doi.org/10.1016/j.desal.2005.02.026.

[49] F.E. Ahmed, R. Hashaikeh, N. Hilal, Hybrid technologies: the future of energy efficient desalination – a review, Desalination 495 (2020), https://doi.org/10.1016/j.desal.2020.114659.

[50] J.A. Fleck, The influence of pressure on boiling water reactor dynamic behavior at atmospheric pressure, Nucl. Sci. Eng. 9 (1961) 271–280, https://doi.org/10.13182/nse61-a15609.

[51] M.C. Georgiou, A.M. Bonanos, J.G. Georgiadis, Evaluation of a multiple-effect distillation unit under partial load operating conditions, Conf. Pap. Energy 2013 (2013) 1–9, https://doi.org/10.1155/2013/482743.

[52] A. Panagopoulos, Process simulation and techno-economic assessment of a zero liquid discharge/multi-effect desalination/thermal vapor compression (ZLD/MED/TVC) system, Int. J. Energy Res. 44 (2020) 473–495, https://doi.org/10.1002/er.4948.

[53] M. Micari, M. Moser, A. Cipollina, B. Fuchs, B. Ortega-Delgado, A. Tamburini, G. Micale, Techno-economic assessment of multi-effect distillation process for the treatment and recycling of ion exchange resin spent brines, Desalination 456 (2019) 38–52, https://doi.org/10.1016/j.desal.2019.01.011.

[54] L.M. Vane, Water recovery from brines and salt-saturated solutions operability and thermodynamic efficiency considerations for desalination technologies, Chem. Technol. Biotechnol. (2017), https://doi.org/10.1002/jctb.5225.

[55] M. Micari, A. Cipollina, A. Tamburini, M. Moser, V. Bertsch, G. Micale, Combined membrane and thermal desalination processes for the treatment of ion exchange resins spent brine, Appl. Energy 254 (2019) 113699, https://doi.org/10.1016/j.apenergy.2019.113699.

[56] B. Van Der Bruggen, K. Everaert, D. Wilms, C. Vandecasteele, Application of nanofiltration for removal of pesticides, nitrate and hardness from ground water: rejection properties and economic evaluation, J. Membr. Sci. 193 (2001) 239–248, https://doi.org/10.1016/S0376-7388(01)00517-8.

[57] U.K. Kesieme, N. Milne, H. Aral, C.Y. Cheng, M. Duke, Economic analysis of desalination technologies in the context of carbon pricing, and opportunities for membrane distillation, Desalination 323 (2013) 66–74, https://doi.org/10.1016/j.desal.2013.03.033.

[58] R. Turton, R.C. Bailie, W.B. Whiting, Analysis, synthesis, and design of chemical processes, 1998, https://doi.org/10.5860/choice.36-0974.

[59] M. Micari, M. Moser, A. Cipollina, A. Tamburini, G. Micale, V. Bertsch, Towards the implementation of circular economy in the water softening industry: a technical, economic and environmental analysis, J. Clean. Prod. 255 (2020) 120291, https://doi.org/10.1016/j.jclepro.2020.120291.

[60] Eurostat, Customs code: 281610, Database: EU trade since 1988 by HS2-4-6 and CN8 (DS-045409). http://epp.eurostat.ec.europa.eu/newxtweb/submitformatselect.do, 2022.

[61] Intratec, Calcium Hydroxide Prices: Current & Historical Data in Several Countries. https://www.intratec.us/chemical-markets/calcium-hydroxide-price?gclid=CjwKCAjw9aiIBhA1EiwAJ_GTSvik9uLcm9I4adTTbpANBGbMg15duTgKCRQIuZv5m4m4YmA0vUZWWhoCXvsQAvD_BwE, 2021.

[62] Intratec, Caustic Soda Prices: Current & Historical Data in Several Countries. https://www.intratec.us/chemical-markets/caustic-soda-price?gclid=CjwKCAjw9aiIBhA1EiwAJ_GTSknGy4TOBaoTVLsviDB3Lfi00vgmUKuFagRDjYIafRrDlarrUHCxABoCCMMQAvD_BwE, 2021.

[63] A. Culcasi, R. Gueccia, S. Randazzo, A. Cipollina, G. Micale, Design of a novel membrane-integrated waste acid recovery process from pickling solution, J. Clean. Prod. 236 (2019), 117623, https://doi.org/10.1016/j.jclepro.2019.117623.

[64] A. Panagopoulos, Techno-economic evaluation of a solar multi-effect distillation/thermal vapor compression hybrid system for brine treatment and salt recovery, Chem. Eng. Process. Process Intensif. 152 (2020), 107934, https://doi.org/10.1016/j.cep.2020.107934.

[65] A. Pérez-González, R. Ibáñez, P. Gómez, A.M. Urtiaga, I. Ortiz, J.A. Irabien, Nanofiltration separation of polyvalent and monovalent anions in desalination brines, J. Membr. Sci. 473 (2015) 16–27, https://doi.org/10.1016/j.memsci.2014.08.045.

[66] K. Mitko, E. Laskowska, M. Turek, P. Dydo, K. Piotrowski, Scaling risk assessment in nanofiltration of mine waters, Membranes (Basel) 10 (2020) 1–18, https://doi.org/10.3390/membranes10100288.

[67] M.E.A. Ali, Nanofiltration process for enhanced treatment of RO brine discharge, Membranes (Basel) 11 (2021) 212, https://doi.org/10.3390/membranes11030212.

[68] Codex Alimentarius Commission, Codex standard for food grade salt. http://www.justice.gov.md/file/Centruldearmonizarealegislatiei/Bazadedate/Materiale2011/Legislatie/CODEXSTAN150-19851CODEXSTANDARDFORFOODGRADESALTCXSTAN.pdf, 2006.

[69] M. Micari, D. Diamantidou, B. Heijman, M. Moser, A. Haidari, H. Spanjers, V. Bertsch, Experimental and theoretical characterization of commercial nanofiltration membranes for the treatment of ion exchange spent regenerant, J. Memb. Sci. 606 (2020), 118117, https://doi.org/10.1016/j.memsci.2020.118117.

[70] Waternet, How much does a cubic metre of water cost?. https://www.waternet.nl/en/veelgestelde-vragen/tap-water/what-does-a-cubic-metre-of-tap-water-cost/, 2021.

[71] ICIS, European economy will be a key driver for HCl in 2020 negotiations. https://www.icis.com/explore/resources/news/2019/11/13/10443560/european-economy-will-be-a-key-driver-for-hcl-in-2020-negotiations, 2021.

[72] Eurostat, Electricity price statistics, Eur. Comm. https://ec.europa.eu/eurostat/statistics-explained/index.php/Electricity_price_statistics, 2020.

[73] T.G. Eschenbach, Spiderplots versus tornado diagrams for sensitivity analysis, Interfaces (Providence) 22 (1992) 40–46, https://doi.org/10.1287/inte.22.6.40.

[74] A. Culcasi, R. Ktori, A. Pellegrino, M. Rodriguez-pascual, M.C.M. Van Loosdrecht, Towards sustainable production of minerals and chemicals through seawater brine treatment using Eutectic freeze crystallization and Electrodialysis with bipolar membranes, J. Clean. Prod. 368 (2022), https://doi.org/10.1016/j.jclepro.2022.133143.

Acronyms

BC: brine concentrator
BCr: brine crystallizer
BMED: electrodialysis with bipolar membranes
BTSC: brine treatment specific cost [€/m^3]
capEX: capital expenditure [€/year]
CEPCI: chemical engineering plant cost index
Cr: crystallizer
DLR: German Aerospace Center
ED: electrodialysis
EDR: electrodialysis reversal
Ev: evaporator
FO: forward osmosis
IEX: ion exchange
LCOC$_{a(OH)2}$: levelized cost of calcium hydroxide [€/ton]
LCOM$_{g(OH)2}$: levelized cost of magnesium hydroxide [€/ton]
LCOS$_{alt}$: levelized cost of salt (NaCl) [€/ton]
LCOW$_{ater}$: levelized cost of water [€/m^3]
MCr: membrane crystallizer
MD: membrane distillation
ME: membrane electrolysis
MED: Multi-Effect Distillation
MLD: Minimal Liquid Discharge
MRC: Magnesium Reactive Crystallizer
MSF: Multi-Stage Flash
NF: Nanofiltration
NTC: NaCl Thermal Crystallizer
opEX: operating expenditure [€/year]
RCE: remote component environment
REV: revenue [€/year]
RED: reverse electrodialysis
RO: reverse osmosis
SED: selective electrodialysis
SWCC: Saline Water Conversion Corporation
SWRO: seawater reverse osmosis
TBT: Top Brine Temperature [°C]
TDS: total dissolved salts [g/L]
TVC: thermal vapour compression
WAIV: wind aided intensified evaporation
ZLD: Zero Liquid Discharge

Greek letters

α: rejection correction factor for bivalent ions
β: rejection correction factor for monovalent ions

Nomenclature

A: area [m^2]
ith: bivalent ionic species
jth: monovalent ionic species
P: pressure [Pa]
Q: mass flow rate [ton/h]
V: volumetric flow rate [m^3/h]
R: NF membrane ion rejection